

A FRAMEWORK FOR MACHINE LEARNING OF MODEL ERROR IN DYNAMICAL SYSTEMS

MATTHEW E. LEVINE AND ANDREW M. STUART

ABSTRACT. The development of data-informed predictive models for dynamical systems is of widespread interest in many disciplines. We present a unifying framework for blending mechanistic and machine-learning approaches to identify dynamical systems from data. We compare pure data-driven learning with hybrid models which incorporate imperfect domain knowledge; we refer to the discrepancy between an assumed truth model and the imperfect mechanistic model as *model error*. We cast the problem in both continuous- and discrete-time, for problems in which the model error is memoryless and in which it has significant memory, and we compare data-driven and hybrid approaches experimentally. Our formulation is agnostic to the chosen machine learning model—any parametric or non-parametric function class can be used within our paradigm.

Using the Lorenz '63 and Lorenz '96 Multiscale systems, we find that hybrid methods substantially outperform solely data-driven approaches, even when the hypothesized (but imperfect) mechanistic model has large discrepancies from the true underlying model; we also find that hybrid methods outperform purely mechanism-driven approaches, even when the hypothesized (but imperfect) mechanistic model makes only small errors in the vector field defining the true dynamics. Moreover, hybrid methods achieve superior accuracy with less training data and fewer parameters than purely data-driven approaches. We also find that, while a continuous-time framing allows for robustness to irregular sampling and desirable domain-interpretability, a discrete-time framing can provide similar or better predictive performance, especially when data are undersampled and the vector field cannot be resolved.

We study model error from the learning theory perspective, defining the excess risk and generalization error; for a linear model of the error used to learn about ergodic dynamical systems, both excess risk and generalization error are bounded by terms that diminish with the square-root of T . We also illustrate scenarios that benefit from modeling with memory, proving that continuous-time recurrent neural networks can, in principle, learn memory-dependent model error and reconstruct the original system arbitrarily well; numerical results are presented to explain some of the challenges in representing memory by this approach. We also connect recurrent neural networks to reservoir computing and thereby relate the learning of memory-dependent error to recent work on supervised learning between Banach spaces using random features.

DEPT. OF COMPUTING AND MATHEMATICAL SCIENCES, CALIFORNIA INSTITUTE OF TECHNOLOGY,
 PASADENA, CA 91125, USA

E-mail addresses: mlevine@caltech.edu, astuart@caltech.edu.

Key words and phrases. Dynamical Systems, Model Error, Statistical Learning, Random Features, Recurrent Neural Networks, Reservoir Computing.

The authors are grateful to David Albers, Oliver Dunbar, Ian Melbourne, and Yisong Yue for helpful discussions. The work of MEL and AMS was supported by NIH RO1 LM012734 “Mechanistic Machine Learning”. MEL is also supported by the National Science Foundation Graduate Research Fellowship under Grant No. DGE-1745301. AMS is also supported by NSF (award AGS-1835860), NSF (award DMS-1818977), the Office of Naval Research (award N00014-17-1-2079), and the AFOSR under MURI award number FA9550-20-1-0358 (Machine Learning and Physics-Based Modeling and Simulation).

1. INTRODUCTION

1.1. Background and Literature Review. The modeling and prediction of dynamical systems and time-series is an important goal in numerous domains, including biomedicine, climatology, robotics, and the social sciences. Traditional approaches to modeling these systems appeal to careful study of their mechanisms, and the design of targeted equations to represent them. These carefully built *mechanistic models* have impacted humankind in numerous arenas, including our ability to land spacecraft on celestial bodies, provide high-fidelity numerical weather prediction, and artificially regulate physiologic processes, through the use of pacemakers and artificial pancreases, for example. This paper focuses on the learning of *model error*: we assume that an imperfect mechanistic model is known, and that data is used to improve it. We introduce a framework for this problem, focusing on distinctions between Markovian and non-Markovian model error, providing a unifying review of relevant literature, developing some underpinning theory related to both the Markovian and non-Markovian settings, and presenting numerical experiments which illustrate our key findings.

To set our work in context, we first review the use of data-driven methods for time-dependent problems, organizing the literature review around four themes comprising Sections 1.1.1 to 1.1.4; these are devoted, respectively, to pure data-driven methods, hybrid methods that build on mechanistic models, non-Markovian models that describe memory, and applications of the various approaches. Having set the work in context, in Section 1.2 we detail the contributions we make, and describe the organization of the paper.

1.1.1. Data-Driven Modeling of Dynamical Systems. A recent wave of machine learning successes in data-driven modeling, especially in imaging sciences, has shown that we can demand even more from existing models, or that we can design models of more complex phenomena than heretofore. Traditional models built from, for example, low order polynomials and/or linearized model reductions, may appear limited when compared to the flexible function approximation frameworks provided by neural networks and kernel methods. Neural networks, for example, have a long history of success in modeling dynamical systems [Narendra and Parthasarathy, 1992, González-García et al., 1998, Krischer et al., 1993, Rico-Martinez et al., 1994, Rico-Martinez et al., 1993, Rico-Martínez et al., 1992, Lagaris et al., 1998] and recent developments in deep learning for operators continue to propel this trend [Lu et al., 2020, Bhattacharya et al., 2020, Li et al., 2021].

The success of neural networks arguably relies on balanced expressivity and generalizability, but other methods also excel in learning parsimonious and generalizable representations of dynamics. A particularly popular methodology is to perform sparse regression over a dictionary of vector fields, including the use of thresholding approaches (SINDy) [Brunton et al., 2016] and L_1 -regularized polynomial regression [Tran and Ward, 2017, Schaeffer et al., 2017, 2018, 2020]. Non-parametric methods, like Gaussian process models [Rasmussen and Williams, 2006], have also been used widely for modeling nonlinear dynamics [Wang et al., 2005, Frigola et al., 2014, Kocijan, 2016, Chkrebti et al., 2016]. While a good choice of kernel is often essential for the success of these methods, recent progress has been made towards automatic hyperparameter tuning via parametric kernel flows [Hamzi and Owhadi, 2021]. Successes with Gaussian process models were also extended to high dimensional

problems by using random feature map approximations [Rahimi and Recht, 2008a] within the context of data-driven learning of parametric partial differential equations and solution operators [Nelsen and Stuart, 2020]. Advancements to data-driven methods based on Koopman operator theory and dynamic mode decomposition have also had significant impact; they offer exciting new possibilities for predicting nonlinear dynamics from data [Tu et al., 2014, Korda et al., 2020, Alexander and Giannakis, 2020].

It is important to consider whether to model in discrete- or continuous-time, as both have potential advantages. The primary positive for continuous-time modeling lies in its flexibility and interpretability. It allows for training on irregularly sampled timeseries; moreover, the learned right-hand-side can be solved numerically at any timestep, and hence used in a variety of applications. Traditional implementations of continuous-time learning require accurate estimation of time-derivatives of the state, but this may be circumvented using approaches that leverage autodifferentiation software [Rubanova et al., 2019, Kaheman et al., 2020] or methods which learn from statistics derived from time-series, such as moments or correlation functions [Schneider et al., 2020]. Discrete-time approaches, on the other hand, are easily deployed when train and test data sample rates are the same. Moreover, they allow for “non-intrusive” model correction, as additions are applied outside of the numerical integrator; this may be relevant for practical integration with complex simulation software.

Both non-parametric and parametric model classes are used in the learning of dynamical systems, with the latter connecting to the former via the representer theorem, when Gaussian process regression [Rasmussen and Williams, 2006] is used [Burov et al., 2020, Gilani et al., 2021, Harlim et al., 2021].

1.1.2. Hybrid Mechanistic and Data-Driven Modeling. Attempts to transform domains that have relied on traditional mechanistic models, by using purely data-driven (i.e. *de novo* or “learn from scratch”) approaches, often fall short. Now, there is a growing recognition by machine learning researchers that these mechanistic models are very valuable [Miller et al., 2021], as they represent the distillation of centuries of data collected in countless studies and interpreted by domain experts. Recent studies have consistently found advantages of hybrid methods that blend mechanistic knowledge and data-driven techniques. Not only do these methods improve predictive performance [Pathak et al., 2018b], but they also reduce data demands [Rackauckas et al., 2020] and improve interpretability and trustworthiness, which is essential for many applications. This is exemplified by work in autonomous drone landing [Shi et al., 2018] and helicopter flying [Rackauckas et al., 2021], as well as predictions for COVID-19 mortality risk [Sottile et al., 2021] and COVID-19 treatment response [Qian et al., 2021].

The question of how best to use the power of data and machine learning to leverage and build upon our existing mechanistic knowledge is thus of widespread current interest. This question and research direction has been anticipated over the last thirty years of research activity at the interface of dynamical systems with machine learning [Rico-Martinez et al., 1994, Wilson and Zorzetto, 1997, Lovelett et al., 2020], and now a critical mass of effort is developing. A variety of studies have been tackling these questions in weather and climate modeling [Kashinath et al., 2021, Farchi et al., 2021]; even in the imaging sciences, where pure machine learning has been spectacularly successful, emerging work shows that incorporating

knowledge of underlying physical mechanisms improves performance in a variety of image recognition tasks [Ba et al., 2019].

As noted and studied by Ba et al. [2019], Freno and Carlberg [2019] and others, there are a few common high-level approaches for blending machine learning with mechanistic knowledge: (1) use machine learning to learn additive residual corrections for the mechanistic model [Saveriano et al., 2017, Shi et al., 2018, Kaheman et al., 2019, Harlim et al., 2021, Farchi et al., 2021]; (2) use the mechanistic model as an input or feature for a machine learning model [Pathak et al., 2018b, Lei et al., 2020, Borra et al., 2020]; (3) use mechanistic knowledge in the form of a differential equation as a final layer in a neural network representation of the solution, or equivalently define the loss function to include approximate satisfaction of the differential equation [Raissi et al., 2019, 2018, Chen et al., 2021, Smith et al., 2020]; and (4) use mechanistic intuition to constrain or inform the machine learning architecture [Haber and Ruthotto, 2017, Maulik et al., 2021]. Many other successful studies have developed specific designs that further hybridize these and other perspectives [Hamilton et al., 2017, Freno and Carlberg, 2019, Yi Wan et al., 2020, Jia et al., 2021]. In addition, parameter estimation for mechanistic models is a well-studied topic in data assimilation, inverse problems, and other mechanistic modeling communities, but recent approaches that leverage machine learning for this task may create new opportunities for accounting for temporal parameter variations [Miller et al., 2020] and unknown observation functions [Linial et al., 2021].

An important distinction should be made between physics-informed *surrogate* modeling and what we refer to as *hybrid* modeling. Surrogate modeling primarily focuses on replacing high-cost, high-fidelity mechanistic model simulations with similarly accurate models that are cheap to evaluate. These efforts have shown great promise by training machine learning models on expensive high-fidelity simulation data, and have been especially successful when the underlying physical (or other domain-specific) mechanistic knowledge and equations are incorporated into the model training [Raissi et al., 2019] and architecture [Maulik et al., 2021]. We use the term hybrid modeling, on the other hand, to indicate when the final learned system involves interaction (and possibly feedback) between mechanism-based and data-driven models [Pathak et al., 2018b].

In this work, we focus primarily on hybrid methods that learn residuals to an imperfect mechanistic model. The benefits of this form of hybrid modeling, which we and many others have observed, are not yet fully understood in a theoretical sense. Intuitively, nominal mechanistic models are most useful when they encode key nonlinearities that are not readily inferred using general model classes and modest amounts of data. Indeed, classical approximation theorems for fitting polynomials, fourier modes, and other common function bases directly reflect this relationship by bounding the error with respect to a measure of complexity of the target function (e.g. Lipschitz constants, moduli of continuity, Sobolev norms, etc.) [DeVore and Lorentz, 1993][Chapter 7]. Recent work by E et al. [2019] provides a priori error bounds for two-layer neural networks and kernel-based regressions, with constants that depend explicitly on the norm of the target function in the model-hypothesis space (a Barron space and a reproducing kernel Hilbert space, resp.). At the same time, problems for which mechanistic models only capture low-complexity trends (e.g. linear) may still be good candidates for hybrid learning (over purely data-driven), as an accurate linear model reduces the parametric burden for the machine-learning

task; this effect is likely accentuated in data-starved regimes. Furthermore, even in cases where data-driven models perform satisfactorily, a hybrid approach may improve interpretability, trustworthiness, and controllability without sacrificing performance.

Hybrid models are often cast in Markovian, memory-free settings where the learned dynamical system (or its learned residuals) are solely dependent on the observed states. This approach can be highly effective when measurements of all relevant states are available or when the influence of the unobserved states is adequately described by a function of the observables. This is the perspective employed by Shi et al. [2018], where they learn corrections to physical equations of motion for an autonomous vehicle in regions of state space where the physics perform poorly—these residual errors are *driven* by un-modeled turbulence during landing, but can be *predicted* using the observable states of the vehicle (i.e. position, velocity, and acceleration). This is also the perspective taken in applications of high-dimensional multiscale dynamical systems, wherein sub-grid closure models parameterize the effects of expensive fine-scale interactions (e.g. cloud simulations) as functions of the coarse variables [Grabowski, 2001, Khairoutdinov and Randall, 2001, Tan et al., 2018, Brenowitz and Bretherton, 2018, O’Gorman and Dwyer, 2018, Rasp et al., 2018, Schneider et al., 2020, Beucler et al., 2021]. The result is a hybrid dynamical system with a physics-based equation defined on the coarse variables with a Markovian correction term that accounts for the effects of the expensive fine scale dynamics.

1.1.3. Non-Markovian Data-Driven Modeling. Unobserved and unmodeled processes are often responsible for model errors that cannot be represented in a Markovian fashion within the observed variables alone. This need has driven substantial advances in memory-based modeling. One approach to this is the use of delay embeddings [Takens, 1981]. These methods are inherently tied to discrete time representations of the data and, although very successful in many applied contexts, are of less value when the goal of data-driven learning is to fit continuous-time models; this is a desirable modeling goal in many settings.

An alternative to understanding memory is via the Mori-Zwanzig formalism, which is a fundamental building block in the presentation of memory and hidden variables and may be employed for both discrete-time and continuous-time models. Although initially developed primarily in the context of statistical mechanics, it provides the basis for understanding hidden variables in dynamical systems, and thus underpins many generic computational tools applied in this setting [Chorin et al., 2000, Zhu et al., 2018, Gouasmi et al., 2017]. It has been successfully applied to problems in fluid turbulence [Duraismy et al., 2019, Parish and Duraismy, 2017] and molecular dynamics [Li et al., 2017, Hijón et al., 2010]. Studies by Ma et al. [2019], Wang et al. [2020] demonstrated how the Mori-Zwanzig formalism motivates the use of recurrent neural networks (RNNs) [Rumelhart et al., 1986, Goodfellow et al., 2016] as a deep learning approach to non-Markovian closure modeling. Indeed, closure modeling using RNNs has become an exciting new way to learn memory-based closures [Kani and Elsheikh, 2017, Chattopadhyay et al., 2020b, Harlim et al., 2021].

In contrast, Lin and Lu [2021] use the Mori-Zwanzig formalism to directly justify a delay-embedding approach to closure modeling. Harlim et al. [2021] performed extensive comparisons between these delay-embedding and RNN-based closure

approaches. Although the original formulation of Mori-Zwanzig as a general purpose approach to modeling partially observed systems was in continuous-time [Chorin et al., 2000], many practical implementations adopt a discrete-time picture [Darve et al., 2009, Lin and Lu, 2021]. This causes the learned memory terms to depend on sampling rates, which, in turn, can inhibit flexibility and interpretability of the model.

Recent advances in continuous-time memory-based modeling, however, may be applicable to these non-Markovian hybrid model settings. The theory of continuous-time RNNs (i.e. formulated as differential equations, rather than a recurrence relation) was studied in the 1990s [Funahashi and Nakamura, 1993, Beer, 1995], albeit for equations with a specific additive structure. This structure was exploited in a continuous-time reservoir computing approach by Lu et al. [2018] for reconstructing chaotic attractors from data; we note that comparisons between RNNs and reservoir computing (a subclass of RNNs with random parameters fixed in the recurrent state) in discrete-time have yielded mixed conclusions in terms of their relative efficiencies and ability to retain memory [Vlachas et al., 2020, Chattopadhyay et al., 2020a]. Recent formulations of continuous-time RNNs have departed slightly from the additive structure, and have focused on constraints and architectures that ensure stability of the resulting dynamical system [Chang et al., 2019, Erichson et al., 2020, Niu et al., 2019, Rubanova et al., 2019, Sherstinsky, 2020]. In addition, significant theoretical work has been performed for linear RNNs in continuous-time [Li et al., 2020]. Nevertheless, these various methods have not yet been formulated within a hybrid modeling framework, nor has their approximation power been carefully evaluated in that context. A recent step in this direction, however, is the work by Gupta and Lermusiaux [2021], which tackles non-Markovian hybrid modeling in continuous-time with neural network-based delay differential equations.

1.1.4. Applications of Data-Driven Modeling. In order to deploy hybrid methods in real-world scenarios, we must also be able to cope with noisy, partial observations. Accommodating the learning of model error in this setting, as well as state estimation, is an active area of research in the data assimilation (DA) community [Pulido et al., 2018, Farchi et al., 2021, Bocquet et al., 2020]. Learning dynamics from noisy data is generally non-trivial for nonlinear systems—there is a chicken-and-egg problem in which accurate state estimation typically relies on the availability of correct models, and correct models are most readily identified using accurate state estimates. Recent studies have addressed this challenge by attempting to jointly learn the noise and the dynamics. Gottwald and Reich [2021] approach this problem from a data assimilation perspective, and employ an Ensemble Kalman Filter (EnKF) to iteratively update the parameters for their dynamics model, then filter the current state using the updated dynamics. Similar studies were performed by Brajard et al. [2021], and applied specifically in model error scenarios [Brajard et al., 2020, Farchi et al., 2021, Wikner et al., 2020]. Kaheman et al. [2019] approached this problem from a variational perspective, performing a single optimization over all noise sequences and dynamical parameterizations. Nguyen et al. [2019] used an Expectation-Maximization perspective to compare these variational and ensemble-based approaches, and further study is needed to understand the trade-offs between these styles of optimization.

We note that these data assimilators are themselves dynamical systems, which can be tuned (using optimization and machine learning) to provide more accurate state

updates and more efficient state identification. However, while learning improved DA schemes is sometimes viewed as a strategy for coping with model error [Zhu and Kamachi, 2000], we see the optimization of DA and the correction of model errors as two separate problems that should be addressed individually.

When connecting models of dynamical systems to real-world data, it is also essential to recognize that available observables may live in a very different space than the underlying dynamics. Recent studies have shown ways to navigate this using autoencoders and dynamical systems models to jointly learn a latent embedding and dynamics in that latent space [Champion et al., 2019]. Proof of concepts for similar approaches primarily focus on image-based inputs, but have potential for applications in medicine [Linial et al., 2021] and reduction of nonlinear partial differential equations [Maulik et al., 2021].

1.2. Our Contributions. Despite this large and recent body of work in data-driven learning methods and hybrid modeling strategies, many challenges remain for understanding how to best combine mechanistic and machine-learned models; indeed, the answer is highly dependent on the application. Here, we construct a mathematical framework that unifies many of the common approaches for blending mechanistic and machine learning models; having done so we provide strong evidence for the value of hybrid approaches. Our contributions are listed as follows:

- (1) We provide an overarching framework for learning model error from data in dynamical systems settings, studying both discrete- and continuous-time models, together with Markovian and memory-dependent representations of the model error. This formulation is agnostic to choice of mechanistic model and class of machine learning functions.
- (2) We study the Markovian learning problem in the context of ergodic continuous-time dynamical systems, proving bounds on the excess risk and generalization error.
- (3) We present a simple approximation theorem for learning memory-dependent (non-Markovian) model error in continuous-time using recurrent neural networks.
- (4) We describe numerical experiments which demonstrate the utility of learning model error in comparison both with pure data-driven learning and with pure (but slightly imperfect) mechanistic modeling.
- (5) We describe numerical experiments comparing the benefits of learning discrete- versus continuous-time models.

In Section 2, we address contribution 1. by defining the general settings of interest for dynamical systems in both continuous- and discrete-time. We then link these underlying systems to a machine learning framework in Sections 3 and 4; in the former we formulate the problem in the setting of statistical learning, and in the latter we define concrete optimization problems found from finite parameterizations of the hypothesis class in which the model error is sought. Section 5 is focused on specific choices of architectures, and underpinning theory for machine learning methods with these choices: we analyze linear methods from the perspective of learning theory in the context of ergodic dynamical systems (contribution 2.); and we describe an approximation theorem for continuous-time hybrid recurrent neural networks (contribution 3.). Finally, Section 6 presents our detailed numerical

experiments; we apply the methods in Section 5 to exemplar dynamical systems of the forms outlined in Section 2, and highlight our findings (contributions 4. and 5.).

2. DYNAMICAL SYSTEMS SETTING

We present a general framework for modeling a dynamical system with Markovian model error, first in continuous-time (Section 2.1) and then in discrete-time (Section 2.2). We then extend the framework to the setting of non-Markovian model error (Section 2.3), including a parameter ε which enables us to smoothly transition from scale-separated problems (where Markovian closure is likely to be accurate) to problems where the unobserved variables are not scale-separated from those observed (where Markovian closure is likely to fail and memory needs to be accounted for). It is important to note that the continuous-time formulation necessarily assumes an underlying data-generating process that is continuous in nature. The discrete-time formulation can be viewed as a discretization of an underlying continuous system, but can also represent systems that are truly discrete.

The settings that we present are all intended to represent and classify common situations that arise in modeling and predicting dynamical systems. In particular, we stress two key features. First, we point out that mechanistic models (later referred to as a vector field f_0 or flow map Ψ_0) are often available and may provide predictions with reasonable fidelity. However, these models are often simplifications of the true system, and thus can be improved with data-driven approaches. Nevertheless, they provide a useful starting point that can reduce the complexity and data-hunger of the learning problems. In this context, we study trade-offs between discrete- and continuous-time framings. While we begin with fully-observed contexts in which the dynamics are Markovian with respect to the observed state x , we later note that we may only have access to partial observations x of a larger system (x, y) . By restricting our interest to prediction of these observables, we show how a latent dynamical process (e.g. a RNN) has the power to reconstruct the correct dynamics for our observables.

2.1. Continuous-Time. Consider the following dynamical system

$$(2.1) \quad \dot{x} = f^\dagger(x), \quad x(0) = x_0,$$

and define $\mathbf{X}_s := C([0, s]; \mathbb{R}^{d_x})$. If $f^\dagger \in C^1(\mathbb{R}^{d_x}; \mathbb{R}^{d_x})$ then (2.1) has solution $x(\cdot) \in \mathbf{X}_T$ for any $T < T_{\max} = T_{\max}(x_0) \in \mathbb{R}^+$, the maximal interval of existence.

The primary model error scenario we envisage in this section is one in which the vector field f^\dagger can only be partially known or accessed: we assume that

$$f^\dagger = f_0 + m^\dagger$$

where f_0 is known to us and m^\dagger is not known. For any $f_0 \in C^1(\mathbb{R}^{d_x}; \mathbb{R}^{d_x})$ (regardless of its fidelity), there exists a function $m^\dagger(x) \in C^1(\mathbb{R}^{d_x}; \mathbb{R}^{d_x})$ such that eq. (2.1) can be rewritten as

$$(2.2) \quad \dot{x} = f_0(x) + m^\dagger(x).$$

However, for this paper, it is useful to think of m^\dagger as being small relative to f_0 ; the function m^\dagger accounts for *model error*. While the approach in (2.2) is targeted at

learning residuals of f_0 , f^\dagger can alternatively be reconstructed from f_0 through a different function $m^\dagger(x) \in C^1(\mathbb{R}^{2d_x}; \mathbb{R}^{d_x})$ using the form

$$(2.3) \quad \dot{x} = m^\dagger(x, f_0(x)).$$

Both approaches are defined on spaces that allow perfect reconstruction of f^\dagger . However, the first formulation hypothesizes that the missing information is additive; the second formulation provides no such indication. Because the first approach ensures substantial usage of f_0 , it has advantages in settings where f_0 is trusted by practitioners and model explainability is important. The second approach will likely see advantages in settings where there is a simple non-additive form of model error, including coordinate transformations and other (possibly state-dependent) nonlinear warping functions of the nominal physics f_0 . Note that the use of f_0 in representing the model error in the augmented-input setting of eq. (2.3) includes the case of not leveraging f_0 at all. It is, hence, potentially more useful than simply adopting an x -dependent model error; but it requires learning a more complex function.

The augmented-input method also has connections to model stacking [Wolpert, 1992]; this perspective can be useful when there are N model hypotheses:

$$\dot{x} = m^\dagger(x, f_0^{(1)}(x), \dots, f_0^{(N)}(x); \theta).$$

Our goal is to use machine learning to approximate these corrector functions m^\dagger using our nominal knowledge f_0 and observations of a trajectory $\{x(t)\}_{t=0}^T \in \mathbf{X}_T$, for some $T < T_{\max}(x_0)$, from the true system (2.1). In this work, we consider only the case of learning $m^\dagger(x)$ in equation (2.2). For now the reader may consider $\{x(t)\}_{t=0}^T$ given without noise so that, in principle, $\{\dot{x}(t)\}_{t=0}^T$ is known and may be leveraged. In practice this will not be the case, for example if the data are high-frequency but discrete in time; we address this issue in what follows.

2.2. Discrete-Time. Consider the following dynamical system

$$(2.4) \quad x_{k+1} = \Psi^\dagger(x_k)$$

and define $\mathbf{X}_K := \ell^\infty(\{0, \dots, K\}; \mathbb{R}^{d_x})$. If $\Psi^\dagger \in C(\mathbb{R}^{d_x}; \mathbb{R}^{d_x})$ the map yields solution $\{x_k\}_{k \in \mathbb{Z}^+} \in \mathbf{X}_\infty := \ell^\infty(\mathbb{Z}^+; \mathbb{R}^{d_x})$.¹ As in the continuous-time setting, we assume we only have access to an approximate mechanistic model $\Psi_0 \in C(\mathbb{R}^{d_x}; \mathbb{R}^{d_x})$. Again, we can correct Ψ_0 using an additive residual term $m^\dagger \in C(\mathbb{R}^{d_x}; \mathbb{R}^{d_x})$ in a model of form

$$(2.5) \quad x_{k+1} = \Psi_0(x_k) + m^\dagger(x_k),$$

or by feeding Ψ_0 as an input to a corrective warping function $m^\dagger \in C(\mathbb{R}^{2d_x}; \mathbb{R}^{d_x})$

$$x_{k+1} = m^\dagger(x_k, \Psi_0(x_k));$$

we focus our experiments on the additive residual framing in eq. (2.5).

Note that the discrete-time formulation can be made compatible with continuous-time data sampled uniformly at rate Δt . To see this, consider eq. (2.1) and its solution operator $\Phi^\dagger(x_0, t) := x(t)$. We then define

$$(2.6) \quad \Psi^\dagger(v) := \Phi^\dagger(v, \Delta t)$$

¹Here we define $\mathbb{Z}^+ = \{0, \dots, \}$, the non-negative integers, including zero.

which can be obtained via numerical integration of f^\dagger . Similarly, we can consider the solution operator Φ_0 defined by the vector field $f_0(x)$ to define a discrete map

$$(2.7) \quad \Psi_0(v) := \Phi_0(v, \Delta t)$$

In these settings, $x(k\Delta t) = x_k$ for $k \in \mathbb{N}$.

2.3. Partially Observed Systems (Continuous-Time). The framework in Sections 2.1 and 2.2 assumes that the system dynamics are Markovian with respect to observable x . Most of our experiments are performed in the fully-observed Markovian case. However, this assumption rarely holds in real-world systems. Consider a block-on-a-spring experiment conducted in an introductory physics laboratory. In principle, the system is strictly governed by the position and momentum of the block (i.e. f_0), along with a few scalar parameters. However (as most students' error analysis reports will note), the dynamics are also driven by a variety of external factors, like a wobbly table or a poorly greased track. The magnitude, timescale, and structure of the influence of these different factors are rarely known; and yet, they are somehow encoded in the discrepancy between the nominal equations of motion and the (noisy) observations of this multiscale system.

Thus we also consider the setting in which the dynamics of x is not Markovian. If we consider x to be the observable states of a Markovian system in dimension higher than d_x , then we can write the full system as

$$(2.8a) \quad \dot{x} = f^\dagger(x, y), \quad x(0) = x_0$$

$$(2.8b) \quad \dot{y} = \frac{1}{\varepsilon} g^\dagger(x, y), \quad y(0) = y_0.$$

Here $f^\dagger \in C^1(\mathbb{R}^{d_x} \times \mathbb{R}^{d_y}; \mathbb{R}^{d_x})$, $g^\dagger \in C^1(\mathbb{R}^{d_x} \times \mathbb{R}^{d_y}; \mathbb{R}^{d_y})$, and $\varepsilon > 0$ is a constant measuring the degree of scale-separation (which is large when ε is small). The system yields solution ² $x(\cdot) \in \mathbf{X}_T, y(\cdot) \in \mathbf{Y}_T$ for any $T < T_{\max}(x(0), y(0)) \in \mathbb{R}^+$, the maximal interval of existence. We view y as the complicated, unresolved, or unobserved aspects of the true underlying system.

For any $f_0 \in C^1(\mathbb{R}^{d_x}; \mathbb{R}^{d_x})$ (regardless of its fidelity), there exists a function $m^\dagger(x, y) \in C^1(\mathbb{R}^{d_x} \times \mathbb{R}^{d_y}; \mathbb{R}^{d_x})$ such that eq. (2.8) can be rewritten as

$$(2.9a) \quad \dot{x} = f_0(x) + m^\dagger(x, y)$$

$$(2.9b) \quad \dot{y} = \frac{1}{\varepsilon} g^\dagger(x, y).$$

Now observe that, by considering the solution of equation (2.9b) as a function of the history of x , the influence of $y(\cdot) \in \mathbf{Y}_t$ on the solution $x(\cdot) \in \mathbf{X}_t$ can be captured by a parameterized (w.r.t. t) family of operators $m_t^\dagger: \mathbf{X}_t \times \mathbb{R}^{d_y} \times \mathbb{R}^+ \mapsto \mathbb{R}^{d_x}$ on the historical trajectory $\{x(s)\}_{s=0}^t$, unobserved initial condition $y(0)$, and scale-separation parameter ε such that

$$(2.10) \quad \dot{x}(t) = f_0(x(t)) + m_t^\dagger(\{x(s)\}_{s=0}^t; y(0), \varepsilon).$$

Our goal is to use machine learning to find a Markovian model, in which x is part of the state variable, using our nominal knowledge f_0 and observations of a

²With \mathbf{Y}_T defined analogously to \mathbf{X}_T .

trajectory $\{x(t)\}_{t=0}^T \in \mathbf{X}_T$, for some $T < T_{\max}(x_0, y_0)$, from the true system (2.8); note that $y(\cdot)$ is not observed and nothing is assumed known about the vector field g^\dagger or the parameter ε .

Note that equations (2.8), (2.9) and (2.10) are all equivalent formulations of the same problem and have identical solutions. The third formulation points towards two intrinsic difficulties: the unknown “function” to be learned is in fact defined by a family of operators m_t^\dagger mapping the Banach space of path history into \mathbb{R}^{d_x} ; secondly the operator is parameterized by $y(0)$ which is unobserved. We will address the first issue by showing that the operators m_t^\dagger can be arbitrarily well-approximated from within a family of differential equations in dimension $\mathbb{R}^{2d_x+d_y}$; the second issue may be addressed by techniques from data assimilation [Asch et al., 2016, Law et al., 2015, Reich and Cotter, 2015] once this approximating family is learned. We emphasize, however, that we do not investigate the practicality of this approach to learning non-Markovian systems and much remains to be done in this area.

It is also important to note that these non-Markovian operators m_t^\dagger can sometimes be adequately approximated by invoking a Markovian model for x and simply learning function $m^\dagger(\cdot)$ as in Section 2.1. For example, when $\varepsilon \rightarrow 0$ and the y dynamics, with x fixed, are sufficiently mixing, the averaging principle [Bensoussan et al., 2011, Vanden-Eijnden and others, 2003, Pavliotis and Stuart, 2008] may be invoked to deduce that

$$\lim_{\varepsilon \rightarrow 0} m_t^\dagger(\{x(s)\}_{s=0}^t; y(0), \varepsilon) = m^\dagger(x(t))$$

for some m^\dagger as in Section 2.1.

It is highly advantageous to identify settings where Markovian modeling is sufficient, as it is a simpler learning problem. We find that learning m_t^\dagger is necessary when there is significant memory required to explain the dynamics of x ; learning m^\dagger is sufficient when memory effects are minimal. In Section 6, we show that Markovian closures can perform well for certain tasks even when the scale-separation factor ε is not small. In Section 3 we demonstrate how the family of operators m_t^\dagger may be represented through ordinary differential equations, appealing to ideas which blend continuous-time RNNs with an assumed known vector field f_0 .

2.4. Partially Observed Systems (Discrete-Time). The discrete-time analog of the previous setting is as follows. We consider mapping

$$(2.11a) \quad x_{k+1} = \Psi_1^\dagger(x_k, y_k)$$

$$(2.11b) \quad y_{k+1} = \Psi_2^\dagger(x_k, y_k)$$

with $\Psi_1^\dagger \in C(\mathbb{R}^{d_x} \times \mathbb{R}^{d_y}; \mathbb{R}^{d_x})$, $\Psi_2^\dagger \in C(\mathbb{R}^{d_x} \times \mathbb{R}^{d_y}; \mathbb{R}^{d_y})$, yielding solutions $\{x_k\}_{k \in \mathbb{Z}^+} \in \mathbf{X}_\infty$ and $\{y_k\}_{k \in \mathbb{Z}^+} \in \mathbf{Y}_\infty$.

As in the continuous-time setting, we assume that while we do not know the full equations $\Psi_1^\dagger, \Psi_2^\dagger$, we do have an approximate model Ψ_0 that is Markovian on the observable x . Hence, we use our available physics Ψ_0 and rewrite eq. (2.11) as

$$(2.12a) \quad x_{k+1} = \Psi_0(x_k) + m^\dagger(x_k, y_k)$$

$$(2.12b) \quad y_{k+1} = \Psi_2^\dagger(x_k, y_k)$$

and can again, analogously to (2.10), write a solution in the space of observables as

$$(2.13) \quad x_{k+1} = \Psi_0(x_k) + m_k^\dagger(\{x_s\}_{s=0}^k, y_0)$$

with $m_k^\dagger: \mathbf{X}_k \times \mathbb{R}^{d_y} \rightarrow \mathbb{R}^{d_x}$, a function of the historical trajectory $\{x_s\}_{s=0}^k$ and the unobserved initial condition y_0 . As shown for continuous-time in (2.10) and for discrete-time in (2.13), the true residual corrector function for f_0 is now a non-Markovian term that depends on the history of the observable state x and initial condition $y(0)$. While this dependence on initial condition y_0 may appear daunting, many applications show substantial memory fading properties that allow for this dependence to be dropped. Indeed if this discrete-time system is computed from the time Δt map for (2.1) then, for $\varepsilon \ll 1$ and when averaging scenarios apply, a memoryless model as in Section 2.2 may be used.

Remark 2.1. While our entire work has focused on immutable mechanistic models f_0 and Ψ_0 , these models typically have tunable parameters. Of course, we can jointly learn parameters for the mechanistic model and closure term. However, the lack of identifiability between modifying the closure and modifying the physics brings up an interesting question in explainability. Future work might focus on decoupling the learning of parameters and closure terms so that maximal expressivity is first squeezed out of the mechanistic model [Plumlee and Joseph, 2017]. This decoupling can be especially important when we are interested in inferring the parameters, whose estimates are biased by unknown model error [Plumlee, 2017].

3. STATISTICAL LEARNING FOR ERGODIC DYNAMICAL SYSTEMS

Here, we present a learning theory framework within which to consider methods for discovering model error from data. We outline the learning theory in a continuous-time Markovian setting (using possibly discretely sampled data), and point to its analogs in discrete-time and non-Markovian settings.

In the discrete-time settings, we assume access to discretely sampled training data $\{x_k = x(k\Delta t)\}_{k=0}^K$, where Δt is a uniform sampling rate and we assume that $K\Delta t = T$. In the continuous-time settings, we assume access to continuous-time training data $\{\dot{x}(t), x(t)\}_{t=0}^T$; Section 6.2 discusses the important practical question of estimating $\dot{x}(t), x(t)$ from discrete (but high frequency) data. In either case, consider the problem of identifying $m \in \mathcal{M}$ (where \mathcal{M} represents the model, or hypothesis, class) that minimizes a loss function quantifying closeness of m to m^\dagger . In the Markovian setting we choose a measure μ on \mathbb{R}^{d_x} and define the loss

$$\mathcal{L}_\mu(m, m^\dagger) := \int_{\mathbb{R}^{d_x}} \|m^\dagger(x) - m(x)\|_2^2 d\mu(x).$$

If we assume that, at the true m^\dagger , $x(\cdot)$ is ergodic with invariant density μ , then we can exchange time and space averages to see that, for an infinitely long trajectory $\{x(t)\}_{t \geq 0}$,

$$\begin{aligned} \mathcal{I}_\infty(m) &:= \lim_{T \rightarrow \infty} \frac{1}{T} \int_0^T \|m^\dagger(x(t)) - m(x(t))\|_2^2 dt \\ &= \int_{\mathbb{R}^{d_x}} \|m^\dagger(x) - m(x)\|_2^2 d\mu(x) \\ &= \mathcal{L}_\mu(m, m^\dagger). \end{aligned}$$

Since we may only have access to a trajectory dataset of finite length T , it is natural to define

$$\mathcal{I}_T(m) := \frac{1}{T} \int_0^T \|m^\dagger(x(t)) - m(x(t))\|_2^2 dt$$

and note that, by ergodicity,

$$\lim_{T \rightarrow \infty} \mathcal{I}_T(m) = \mathcal{L}_\mu(m, m^\dagger).$$

Finally, we can use eq. (2.2) to get

$$(3.1) \quad \mathcal{I}_T(m) = \frac{1}{T} \int_0^T \|\dot{x}(t) - f_0(x(t)) - m(x(t))\|_2^2 dt.$$

This, possibly regularized, is a natural loss function to employ when continuous-time data is available, and should be viewed as approximating $\mathcal{L}_\mu(m, m^\dagger)$.

We can use these definitions to frame the problem of learning model error in the language of statistical learning [Vapnik, 2013]. If we let \mathcal{M} denote the hypothesis class over which we seek to minimize $\mathcal{I}_T(m)$ then we may define

$$m_\infty^* = \operatorname{argmin}_{m \in \mathcal{M}} \mathcal{L}_\mu(m, m^\dagger) = \operatorname{argmin}_{m \in \mathcal{M}} \mathcal{I}_\infty(m), \quad m_T^* = \operatorname{argmin}_{m \in \mathcal{M}} \mathcal{I}_T(m).$$

The *risk* associated with seeking m^\dagger from the class \mathcal{M} is defined by $\mathcal{L}_\mu(m_\infty^*, m^\dagger)$, noting that this is 0 if $m^\dagger \in \mathcal{M}$. The risk measures the intrinsic error incurred by seeking to learn m^\dagger from the restricted class \mathcal{M} , which typically does not include m^\dagger ; it is an approximation theoretic concept which encodes the richness of the hypothesis class \mathcal{M} . The risk may be decreased by increasing the expressiveness of \mathcal{M} . Thus risk is independent of the data employed. To quantify the effect of data volume on learning m^\dagger , it is helpful to introduce the following two concepts. The *excess risk* is defined by

$$R_T := \mathcal{I}_\infty(m_T^*) - \mathcal{I}_\infty(m_\infty^*)$$

and represents the additional approximation error incurred by using data defined over a finite time horizon T in the estimate of the function m^\dagger . The *generalization error* is

$$G_T := \mathcal{I}_T(m_T^*) - \mathcal{I}_\infty(m_T^*)$$

and represents the discrepancy between training error, which is defined using a finite trajectory, and idealized test error, which is defined using an infinite length trajectory (or, equivalently, the invariant measure μ), when evaluated at the estimate of the function m^\dagger obtained from finite data. We return to study excess risk and generalization error in the context of linear models for m^\dagger , and under ergodicity assumptions on the data generating process, in Section 5.2.

We have introduced a machine learning framework in the continuous-time Markovian setting, but it may be adopted in discrete-time and in non-Markovian settings. In Section 4, we define appropriate objective functions for each of these cases.

Remark 3.1. The developments we describe here for learning in ordinary differential equations can be extended to the case of learning stochastic differential equations; see [Bento et al., 2011, Kutoyants, 2004]. In that setting, consistency in the large T limit is well-understood. It would be interesting to build on the learning theory perspective described here to study statistical consistency for ordinary differential equations; the approaches developed in the work by McGoff et al. [2015], Su and Mukherjee [2021] are potentially useful in this regard.

4. PARAMETERIZATION OF THE LOSS FUNCTION

In this section, we define explicit optimizations for learning (approximate) model error functions m^\dagger for the Markovian settings, and model error operators m_t^\dagger for the non-Markovian settings; both continuous- and discrete-time formulations are given. We defer discussion of specific approximation architectures to the next section. Here we make a notational transition from optimization over (possibly non-parametric) functions $m \in \mathcal{M}$ to functions parameterized by θ that characterize the class \mathcal{M} .

In all the numerical experiments in this paper, we study the use of continuous- and discrete-time approaches to model data generated by a continuous-time process. The set-up in this section reflects this setting, in which two key parameters appear: T , the continuous-time horizon for the data; and Δt , the frequency of the data. The latter parameter will always appear in the discrete-time models; but it may also be implicit in continuous-time models which need to infer continuous time quantities from discretely sampled data. We relate T and Δt by $K\Delta t = T$. We present the general forms of $\mathcal{J}_T(\theta)$ (with optional regularization terms $R(\theta)$). Optimization via derivative-based methodology requires either analytic differentiation of the dynamical system model with respect to parameters, or the use of autodifferentiable ordinary differential equation solvers [Rubanova et al., 2019].

4.1. Continuous-Time Markovian Learning. Here, we approximate the Markovian closure term in (2.2) with a parameterized function $m(x; \theta)$. Assuming full knowledge of $\dot{x}(t), x(t)$, we learn the correction term for the flow field by minimizing the following objective function of θ :

$$(4.1) \quad \mathcal{J}_T(\theta) = \frac{1}{T} \int_0^T \|\dot{x}(t) - f_0(x(t)) - m(x(t); \theta)\|^2 dt + R(\theta)$$

Note that $\mathcal{J}_T(\theta) = \mathcal{I}_T(m(\cdot; \theta)) + R(\theta)$.

Notable examples that leverage this framing include: the paper [Kaheman et al., 2019], where θ are coefficients for a library of low-order polynomials and $R(\theta)$ is a sparsity-promoting regularization defined by the SINDy framework; the paper [Shi et al., 2018], where θ are parameters of a deep neural network and $R(\theta)$ encodes constraints on the Lipschitz constant for m provided by spectral normalization; and the paper [Watson, 2019] which applies this approach to the Lorenz '96 Multiscale system using neural networks with an L_2 regularization on the weights.

4.2. Discrete-Time Markovian Learning. Here, we learn the Markovian correction term in (2.5) for the discrete solution map Ψ_0 by minimizing:

$$(4.2) \quad \mathcal{J}_T(\theta) = \frac{1}{K} \sum_{k=0}^{K-1} \|x_{k+1} - \Psi_0(x_k) - m(x_k; \theta)\|^2 + R(\theta)$$

(Recall that $K\Delta t = T$.) This is the natural discrete-time analog of (4.1) and may be derived analogously, starting from a discrete analog of the loss $\mathcal{L}_\mu(m, m^\dagger)$ where now μ is assumed to be an ergodic measure for (2.4). If a discrete analog of (3.1) is defined, then parameterization of m , and regularization, leads to (4.2). This is the underlying model assumption in the work by Farchi et al. [2021].

4.3. Continuous-Time Non-Markovian Learning. We can attempt to recreate the dynamics in x for eq. (2.10) by modeling the non-Markovian residual term. A common approach is to augment the dynamics space with a variable $r \in \mathbb{R}^{d_r}$ as follows:

$$(4.3a) \quad \dot{x} = f_0(x) + f_1(r, x; \theta)$$

$$(4.3b) \quad \dot{r} = f_2(r, x; \theta)$$

where we seek a d_r large enough and parametric models $\{f_j(r, x; \cdot)\}_{j=1}^2$ expressive enough such that the dynamics in x are reproduced by eq. (4.3). We learn a good parameterization for eq. (4.3) by minimizing the following objective:

$$(4.4) \quad \mathcal{J}_T(\theta) = \frac{1}{T} \int_0^T \|\dot{x}(t) - f_0(x(t)) - f_1(r, x(t); \theta)\|^2 dt + R(\theta)$$

s.t. $r(t)$ solves eq. (4.3b).

Specific functional forms of f_1, f_2 (and their corresponding parameter inference strategies) reduce eq. (4.3) to various approaches. For the continuous-time RNN structure we discuss in the next section we choose f_1 to be linear in r and independent of x , whilst f_2 is a neural network; we may generalize and consider latent ordinary differential equations in which f_1 and f_2 are both neural networks. It is intuitive that the latter may be more expressive and afford a smaller d_r than the former. To our knowledge, studies of continuous-time non-Markovian closures using RNNs have not yet been published; this appears to be a direction that would be interesting to pursue further and we will discuss it from a theoretical standpoint in Section 5.

Remark 4.1. The recent paper [Gupta and Lermusiaux, 2021] proposes an interesting, and more computationally tractable, approach to learning model error in the presence of memory. They propose to learn a closure operator $m_\tau(\cdot; \theta): \mathbf{X}_\tau \rightarrow \mathbb{R}^{d_x}$ for a delay differential equation with finite memory τ :

$$(4.5) \quad \dot{x}(t) = f_0(x(t)) + m_\tau(\{x(t-s)\}_{s=0}^\tau; \theta);$$

neural networks are used to learn the operator m_τ . Alternatively, Gaussian processes were used to fit a specific stochastic generalization of the delay differential equation (4.5) in [Schneider et al., 2020].

4.4. Discrete-Time Non-Markovian Learning. Here, we aim to recreate the dynamics in x for eq. (2.13) by modeling the non-Markovian residual term, and do this by augmenting the dynamics space with a variable $r \in \mathbb{R}^{d_r}$ as follows:

$$(4.6a) \quad x_{k+1} = \Psi_0(x_k) + \Psi_1(r_k, x_k; \theta)$$

$$(4.6b) \quad r_{k+1} = \Psi_2(r_k, x_k; \theta)$$

where we seek a d_r large enough and $\{\Psi_j(r, x; \cdot)\}_{j=1}^2$ expressive enough such that the dynamics in x are reproduced by eq. (4.6). Learning is performed by minimizing the following objective

$$\begin{aligned}
(4.7) \quad \mathcal{J}_T(\theta) &= \frac{1}{K} \sum_{k=0}^{K-1} \|x_{k+1} - \Psi_0(x_k) - \Psi_1(r_k, x_k; \theta)\|^2 + R(\theta) \\
\text{s.t.} \quad \{r_k\}_{k=0}^{K-1} &\text{ solves eq. (4.6b).}
\end{aligned}$$

(Recall that $K\Delta t = T$.) The functional form of Ψ_1, Ψ_2 (and their corresponding parameter inference strategies) reduce eq. (4.6) to various approaches, including recurrent neural networks, latent ordinary differential equations, and delay-embedding maps (e.g. to get a delay embedding map, Ψ_2 is a shift operator). Pathak et al. [2018b] used reservoir computing (a random features approach to RNN, described in the next section) with L_2 regularization to study an approach similar to eq. (4.6), but included $\Psi_0(x_k)$ as a feature in Ψ_1 and Ψ_2 instead of using it as the central model upon which to learn residuals. The data-driven super-parameterization approach in [Chattopadhyay et al., 2020b] also appears to follow the underlying assumption of eq. (4.6).

4.5. Connections to Physics-Informed Neural Networks. It is also of interest to consider how physics-based regularization ideas from Physics-informed Neural Networks (PINNs) [Raissi et al., 2019], which were designed to improve partial differential equation surrogate modeling, can be leveraged for modeling ordinary differential equations. Investigation into this topic is still ongoing [Tipireddy et al., 2019, Yazdani et al., 2020, Antonelo et al., 2021]. A natural starting point is to consider the objective function

$$(4.8) \quad \mathcal{J}_T(\theta) = \frac{1}{T} \int_0^T \left(\|\dot{x} - f(x; \theta)\|^2 + \lambda \|f_0(x) - f(x; \theta)\|^2 \right) dt;$$

however, if the trajectory is not long enough to cover all relevant parts of state-space required for prediction, an alternative is to consider the objective function

$$(4.9) \quad \mathcal{J}_T(\theta) = \frac{1}{T} \int_0^T \|\dot{x} - f(x; \theta)\|^2 dt + \lambda \frac{1}{|X|} \int_X \|f_0(x) - f(x; \theta)\|^2 dx;$$

here X defines a bounded region in Euclidean space to which the dynamics to be learned is assumed to be confined. In both these settings regularization parameter λ can be learned e.g. by via cross-validation. It may be desirable to fit a discrete-time model, given imperfect continuous time vector field, in which case a natural objective function is

$$\begin{aligned}
(4.10) \quad \mathcal{J}_T(\theta) &= \frac{1}{K} \sum_{k=0}^{K-1} \|x_{k+1} - \Psi(x_k; \theta)\|^2 + \frac{\lambda}{L} \sum_{l=0}^{L-1} \left\| f_0(x_l) - \frac{1}{\Delta t} (\Psi(x_l; \theta) - I) \right\|^2.
\end{aligned}$$

Again the second term may be generalized to an integral over space rather than time, if the trajectory data does not explore enough of the state-space. These physics-based regularizations may be especially useful when available data are limited or when derivatives are poorly estimated from data; regularization with respect to deviations from f_0 provides cheap, approximate data augmentation.

5. UNDERPINNING THEORY

In this section we identify specific hypothesis classes \mathcal{M} . We do this using random feature maps [Rahimi and Recht, 2008a] in the Markovian settings (Section 5.1), and using recurrent neural networks in the memory-dependent setting. We then discuss these problems from a theoretical standpoint. In Section 5.2 we study excess risk and generalization error in the context of linear models (a setting which includes the random features model as a special case). And we conclude by discussing the use of RNNs [Goodfellow et al., 2016][Chapter 10] for the non-Markovian settings (discrete- and continuous-time) in Section 5.3; we present an approximation theorem for continuous-time hybrid RNN models. Throughout this section, the specific use of random feature maps and of recurrent neural networks is for illustrative purposes only; other models could, of course, be used.

5.1. Markovian Modeling with Random Feature Maps. In principle, any hypothesis class can be used to learn m^\dagger . However, we focus on models that are easily trained on large-scale complex systems and yet have proven approximation power for functions between finite-dimensional Euclidean spaces. For the Markovian modeling case, we use random feature maps; like traditional neural networks, they possess arbitrary approximation power [Rahimi and Recht, 2008c,b], but further benefit from a quadratic minimization problem in the training phase, as do kernel or Gaussian process methods. In our case studies, we found random feature models sufficiently expressive, we found optimization easily implementable, and we found the learned models generalized well. Moreover, their linearity with respect to unknown parameters enables a straightforward analysis of excess risk and generalization error in Section 5.2. Details on the derivation and specific design choices for our random feature modeling approach can be found in Section 8.3, where we explain how we sample D random feature functions $\varphi : \mathbb{R}^{d_x} \rightarrow \mathbb{R}$ and stack them to form a vector-valued feature map $\phi(x) : \mathbb{R}^{d_x} \rightarrow \mathbb{R}^D$. Given this random function ϕ , we define the hypothesis class

$$(5.1) \quad \mathcal{M} = \{m : \mathbb{R}^{d_x} \rightarrow \mathbb{R}^{d_x} \mid \exists C \in \mathbb{R}^{d_x \times D} : m(x) = C\phi(x)\}.$$

When studying statistical learning, we will also consider the hypothesis class

$$(5.2) \quad \mathcal{M} = \{m : \mathbb{R}^{d_x} \rightarrow \mathbb{R}^{d_x} \mid \exists \theta \in \mathbb{R}^p : m(x) = \sum_{\ell=1}^p \theta_\ell f_\ell(x)\}$$

where the $\{f_\ell\}$ are i.i.d. draws of function ϕ in the case $D = d_x$.

5.1.1. Continuous-Time. In the continuous-time framing, our Markovian closure model uses hypothesis class (5.1) and thus takes the form

$$\dot{x} = f_0(x) + C\phi(x(t)).$$

We rewrite eq. (4.1) for this particular case with an L_2 regularization parameter $\lambda \in \mathbb{R}^+$:

$$(5.3) \quad \mathcal{J}_T(C) = \frac{1}{2T} \int_0^T \|\dot{x}(t) - f_0(x(t)) - C\phi(x(t))\|^2 dt + \frac{\lambda}{2} \|C\|^2.$$

We employ the notation $A \otimes B := AB^T$ for the outer-product between matrices $A \in \mathbb{R}^{m \times n}$, $B \in \mathbb{R}^{l \times n}$, and the following notation for time-average

$$\overline{A}_T := \frac{1}{T} \int_0^T A(t) dt$$

of $A \in L^1([0, T], \mathbb{R}^{m \times n})$. Equation (5.3) is quadratic and convex in C and thus is globally minimized for the unique C^* which makes the derivative of \mathcal{J}_T zero. Consequently, the minimizer C^* satisfies the following linear equation (derived in the Appendix Section 8.4):

$$(5.4) \quad (Z + \lambda I)(C^*)^T = Y.$$

Here, $I \in \mathbb{R}^{D \times D}$ is the identity and

$$(5.5) \quad \begin{aligned} Z &= \overline{[\phi \otimes \phi]}_T \in \mathbb{R}^{D \times D}, \\ Y &= \overline{[\phi \otimes m^\dagger]}_T \in \mathbb{R}^{D \times d_x}. \end{aligned}$$

Of course m^\dagger is not known, but $m^\dagger(t) = \dot{x}(t) - f_0(x(t))$ can be computed from data.

To summarize, the algorithm proceeds as follows: 1) create a realization of random feature vector ϕ ; 2) compute the integrals in eq. (5.5) to obtain Z, Y ; and 3) solve the linear matrix equation eq. (5.4) for C^* . Together this leads to our approximation $m^\dagger(x) \approx m_T^*(x; \theta) := C^* \phi(x)$.

5.1.2. Discrete-Time. In the discrete-time framing, our Markovian closure model takes the form

$$x_{k+1} = \Psi_0(x_k) + C\phi(x_k).$$

We rewrite eq. (4.2) for this particular case with an L_2 regularization parameter $\lambda \in \mathbb{R}^+$:

$$(5.6) \quad \mathcal{J}_T(\theta) = \frac{1}{K} \sum_{k=0}^{K-1} \|x_{k+1} - \Psi_0(x_k) - C\phi(x_k)\|^2 + \frac{\lambda}{2} \|C\|^2.$$

Equation (5.6) is quadratic in C and thus is globally minimized at C^* which satisfies the following linear equation:

$$(5.7) \quad (Z + \lambda I)(C^*)^T = Y.$$

Here

$$(5.8) \quad \begin{aligned} Z &= \frac{1}{K} \sum_{k=0}^{K-1} \phi(x_k) [\phi(x_k)]^T \\ Y &= \frac{1}{K} \sum_{k=0}^{K-1} \phi(x_k) [m^\dagger(x_k)]^T. \end{aligned}$$

The derivation is analogous to that for the continuous time setting, as detailed in Section 8.4. Of course $m^\dagger(\cdot)$ is not known, but $m^\dagger(x_k) = x_{k+1} - \Psi_0(x_k)$ and so Y may be calculated from data. This formulation closely mirrors the fully data-driven linear regression approach in [Gottwald and Reich, 2021]. By computing Z, Y and solving the linear equation eq. (5.7) for C^* , we obtain our approximation $m^\dagger(x) \approx m_T^*(x; \theta) := C^* \phi(x)$.

5.2. Learning Theory for Markovian Models with Linear Hypothesis Class.

In this subsection we provide estimates of the excess risk and generalization error in the context of learning m^\dagger in (2.2) from a trajectory over time horizon T . We study ergodic continuous-time models in the setting of Section 4.1 and seek to learn from the hypothesis class \mathcal{M} defined in (5.2). Here $f_\ell: \mathbb{R}^{d_x} \rightarrow \mathbb{R}^{d_x}$ and $\theta_\ell \in \mathbb{R}$. For the learning theory presented in this subsection, it is not necessary to use the random features construction of the $\{f_\ell\}$; however, we note that, in that setting, universal approximation for random features [Rahimi and Recht, 2008a] shows that the loss function \mathcal{I}_∞ may be made arbitrarily small by choice of p large enough and appropriate choice of parameters. We also note that the theory we present in this subsection is also readily generalized to working with hypothesis class (5.1).

We make the following ergodicity assumption about the data generation process:

Assumption A1. Equation (2.2) possesses a compact global attractor \mathcal{A} supporting invariant measure μ . Furthermore the dynamical system on \mathcal{A} is ergodic with respect to μ and satisfies a central limit theorem of the following form: for all Hölder continuous bounded $\varphi: \mathbb{R}^{d_x} \mapsto \mathbb{R}$, there is $\sigma^2 = \sigma^2(\varphi)$ such that

$$(5.9) \quad \sqrt{T} \left(\frac{1}{T} \int_0^T \varphi(x(t)) dt - \int_{\mathbb{R}^{d_x}} \varphi(x) \mu(dx) \right) \Rightarrow N(0, \sigma^2)$$

where \Rightarrow denotes convergence in distribution with respect to $x(0) \sim \mu$. Furthermore, almost surely with respect to $x(0) \sim \mu$,

$$(5.10) \quad \limsup_{T \rightarrow \infty} \left(\frac{T}{\log \log T} \right)^{\frac{1}{2}} \left(\frac{1}{T} \int_0^T \varphi(x(t)) dt - \int_{\mathbb{R}^{d_x}} \varphi(x) \mu(dx) \right) = \sigma.$$

Remark 5.1. In the work of Melbourne and co-workers, such an assumption is proven to hold for a class of differential equations, including the Lorenz '63 model at, and in a neighbourhood of, the classical parameter values: in [Holland and Melbourne, 2007] the central limit theorem is established; and in [Bahsoun et al., 2020] the continuity of σ in φ is proven. Whilst it is in general very difficult to prove such results for any given chaotic dynamical system, there is strong empirical evidence for such results in many chaotic dynamical systems that arise in practice. This combination of theory and empirical evidence justify studying the learning of model error under Assumption A1. Tran and Ward [2017] were the first to make use of the theory of Melbourne and coworkers to study learning of chaotic differential equations from time-series.

Given m from hypothesis class (5.2) we define

$$(5.11) \quad \theta_\infty^* = \operatorname{argmin}_{\theta \in \mathbb{R}^p} \mathcal{I}_\infty(m(\cdot; \theta)) = \operatorname{argmin}_{\theta \in \mathbb{R}^p} \mathcal{L}_\mu(m(\cdot; \theta))$$

and

$$(5.12) \quad \theta_T^* = \operatorname{argmin}_{\theta \in \mathbb{R}^p} \mathcal{I}_T(m(\cdot; \theta)).$$

(Regularization is not needed in this setting because the data is plentiful—a continuous-time trajectory—and the number of parameters is finite.) Then $\theta_\infty^*, \theta_T^*$ solve the linear systems

$$A_\infty \theta_\infty^* = b_\infty, \quad A_T \theta_T^* = b_T$$

where

$$\begin{aligned} (A_\infty)_{ij} &= \int_{\mathbb{R}^{d_x}} \langle f_i(x), f_j(x) \rangle \mu(dx), & (b_\infty)_j &= \int_{\mathbb{R}^{d_x}} \langle m^\dagger(x), f_j(x) \rangle \mu(dx), \\ (A_T)_{ij} &= \frac{1}{T} \int_0^T \langle f_i(x(t)), f_j(x(t)) \rangle dt, & (b_T)_j &= \frac{1}{T} \int_0^T \langle m^\dagger(x(t)), f_j(x(t)) \rangle dt. \end{aligned}$$

These facts can be derived analogously to the derivation in Section 8.4. Given θ_∞^* and θ_T^* we also define

$$m_\infty^* = m(\cdot; \theta_\infty^*), \quad m_T^* = m(\cdot; \theta_T^*).$$

Recall that it is assumed that f^\dagger, f_0 , and m^\dagger are C^1 . We make the following assumption regarding the vector fields defining hypothesis class \mathcal{M} .

Assumption A2. The functions $\{f_\ell\}_{\ell=0}^p$ are Hölder continuous on \mathbb{R}^{d_x} . In addition, the matrix A_∞ is invertible.

Theorem 5.2. *Let Assumptions A1 and A2 hold. Then the scaled excess risk $\sqrt{T}R$ (resp. scaled generalization error $\sqrt{T}|G|$) is bounded above by $\|\mathcal{E}_R\|$ (resp. $\|\mathcal{E}_G\|$), where random variable $\mathcal{E}_R \in \mathbb{R}^p$ (resp. $\mathcal{E}_G \in \mathbb{R}^{p+1}$) converges in distribution to $N(0, \Sigma_R)$ (resp. $N(0, \Sigma_G)$) w.r.t. $x(0) \sim \mu$. Furthermore, there is constant $C > 0$ such that, almost surely w.r.t. $x(0) \sim \mu$,*

$$\limsup_{T \rightarrow \infty} \left(\frac{T}{\log \log T} \right)^{\frac{1}{2}} (R + |G|) \leq C.$$

The proof is provided in the appendix Section 8.1.

Remark 5.3. The convergence in distribution shows that, with high probability with respect to initial data, the excess risk and the generalization error are bounded above by terms of size $1/\sqrt{T}$. This can be improved to give an almost sure result, at the cost of the factor of $\sqrt{\log \log T}$. The theorem shows that (ignoring log factors and acknowledging the probabilistic nature of any such statements) trajectories of length $\mathcal{O}(\epsilon^{-2})$ are required to produce bounds on the excess risk and generalization error of size $\mathcal{O}(\epsilon)$. In turn, the bounds on excess risk and generalization error also show that empirical risk minimization (of \mathcal{I}_T) approaches the theoretically analyzable concept of risk minimization (of \mathcal{I}_∞) over hypothesis class (5.2). The sum of the excess risk and the generalization error gives

$$E_T := \mathcal{I}_T(m_T^*) - \mathcal{I}_\infty(m_\infty^*).$$

We note that $\mathcal{I}_T(m_T^*)$ is computable, once the approximate solution m_T^* has been identified; thus, when combined with an estimate for E_T , this leads to an estimate for the risk associated with the hypothesis class used. Work by Zhang et al. [2021] demonstrates that error bounds on learned model error terms can be extended to bound error on reproduction of invariant statistics for ergodic Itô diffusions (a generalization of the ordinary differential equation setting we have presented). Moreover, E et al. [2019] provide a direction for proving similar bounds on model error learning using nonlinear function classes (e.g. two-layer neural networks).

Finally we remark on the dependence of the risk and generalization error bounds on the size of the model error. It is intuitive that the amount of data required to learn model error should decrease as the size of the model error decreases. This is demonstrated numerically in Section 6.4 (c.f. Figures 2a and 2b). Here we comment that Theorem 5.2 also exhibits this feature: examination of the proof in Appendix

8.1 shows that all upper bounds on terms appearing in the excess and generalization error are proportional to m^\dagger itself or to m_∞^* , its approximation given an infinite amount of data; note that $m_\infty^* = m^\dagger$ if the hypothesis class contains the truth.

5.3. Non-Markovian Modeling with Recurrent Neural Networks. Recurrent Neural Networks (RNNs) are one of the *de facto* tools for modeling systems with memory. Here, we show straightforward residual implementations of RNNs for continuous- and discrete-time, with the goal of modeling non-Markovian model error. For example, in discrete-time, the form in eq. (4.6) can be specified as

$$(5.13a) \quad x_{k+1} = \Psi_0(x_k) + Cr_k$$

$$(5.13b) \quad r_{k+1} = \sigma(Ar_k + Bx_k + c).$$

The parameters A, B, C, c can be learned to describe memory-dependent model error. Note that inherent in choosing these matrices A, B, C and vector c is a choice of embedding dimension for variable r ; this will typically be larger than dimension of y itself. The goal is to choose them so that output $\{x_k\}_{k=0}^K$ matches output of (2.12), without observation of $\{y_k\}_{k=0}^K$ or knowledge of m^\dagger and Ψ_2^\dagger . We note here that more sophisticated variants, such as Long-Short Term Memory RNNs [Hochreiter and Schmidhuber, 1997], are often more effective, but similar in nature. In continuous-time, we specify the form in eq. (4.3) as

$$(5.14a) \quad \dot{x} = f_0(x) + Cr$$

$$(5.14b) \quad \dot{r} = \sigma(Ar + Bx + c).$$

The goal is to choose A, B, C, c so that output $\{x(t)\}_{t \geq 0}$ matches output of (2.9), without observation of $\{y(t)\}_{t \geq 0}$ or knowledge of m^\dagger and g^\dagger . As in discrete-time, inherent in choosing these matrices A, B, C and vector c is a choice of embedding dimension for variable r which will typically be larger than dimension of y itself.

In both continuous- and discrete-time settings, the idea is to create a recurrent state r of sufficiently large dimension N whose evolution equation takes x as input and, after a final linear transformation, approximates the missing dynamics $m^\dagger(x, y)$. A full discussion of implementation of this model is beyond the scope of this paper. We refer readers to [Goodfellow et al., 2016] for background on discrete RNN implementations and backpropagation through time (BPTT). For implementations of continuous-time RNNs, it is common to leverage the success of the automatic BPTT code written in PyTorch and Tensorflow by discretizing eq. (5.14) with an ordinary differential equation solver that is compatible with these autodifferentiation tools (e.g. `torchdiffeq` [Rubanova et al., 2019]). This compatibility can also be achieved by use of explicit Runge-Kutta schemes [Queiruga et al., 2020]. Note that the discretization of eq. (5.14) can (and perhaps should) be much finer than the data sampling rate Δt , but that this requires reliable estimation of $x(t), \dot{x}(t)$ from discrete data.

Existing approximation theory for discrete-time RNNs [Schäfer and Zimmermann, 2007] can be used to show that eq. (5.13) can approximate discrete-time systems arbitrarily well. However, the approximation theorem for continuous-time RNNs was proved for additive-style equations [Funahashi and Nakamura, 1993]; we extend the result to a more common (non-additive) form, and do so in the context of residual-based learning as in eq. (5.14).

We state the theorem after making three assumptions upon which it rests:

Assumption A3. Functions $f^\dagger, g^\dagger, f_0$ are all globally Lipschitz.

Note that this implies that m^\dagger is also globally Lipschitz.

Assumption A4. Let $\sigma_0 \in C^1(\mathbb{R}; \mathbb{R})$ be bounded and monotonic, with bounded first derivative. Then $\sigma(u)$ defined by $\sigma(u)_i = \sigma_0(u_i)$ satisfies $\sigma \in C^1(\mathbb{R}^p; \mathbb{R}^p)$.

Assumption A5. Fix $T > 0$. There exist $\rho_0, \rho_T \in \mathbb{R}^{d_x} \times \mathbb{R}^{d_y}$ such that, for equation (2.9), $(x(0), y(0)) \in B(0, \rho_0)$ implies that $(x(t), y(t)) \in B(0, \rho_T) \forall t \in [0, T]$.

Theorem 5.4. *Let Assumptions A3-A5 hold. Fix any $T > 0$ and $\rho_0 > 0$, let $x(\cdot), y(\cdot)$ denote the solution of eq. (2.9) with $\varepsilon = 1$ and let $x_\delta(\cdot), r_\delta(\cdot)$ denote the solution of eq. (5.14) with parameters $\theta = \theta_\delta$. Then, for any $\delta > 0$ and any $T > 0$, there is embedding dimension N_δ and parameterization $\theta_\delta = \{A_\delta, B_\delta, C_\delta, c_\delta\}$ with the property that, for any initial condition $(x(0), y(0)) \in B(0, \rho_0)$ for eq. (2.9), there is initial condition $(x_\delta(0), r_\delta(0)) \in \mathbb{R}^{d_x + N_\delta}$ for eq. (5.14), such that*

$$\sup_{t \in [0, T]} \|x - x_\delta\| \leq \delta.$$

The complete proof is provided in the appendix Section 8.2; here we describe its basic structure. Define $m(t) := m^\dagger(x(t), y(t))$ and, with the aim of finding a differential equation for $m(t)$, recall eq. (2.9) with $\varepsilon = 1$ and make the vector field

$$h^\dagger(x, y) := \nabla_x m^\dagger(x, y)[f_0(x) + m^\dagger(x, y)] + \nabla_y m^\dagger(x, y)g^\dagger(x, y).$$

Then, for solutions to eq. (2.9), we have

$$\dot{m} = \frac{d}{dt}m^\dagger(x, y) = h^\dagger(x, y).$$

Thus we deduce that the variables (x, y, m) satisfy the equations

$$(5.15a) \quad \dot{x} = f_0(x) + m$$

$$(5.15b) \quad \dot{y} = g^\dagger(x, y)$$

$$(5.15c) \quad \dot{m} = h^\dagger(x, y).$$

Here $m(t)$ must be initialized at $m^\dagger(x(0), y(0))$ to ensure equivalence between the solution of (5.15) and (2.9). Under this assumption on the initialization, the manifold $m = m^\dagger(x, y)$ is invariant for (5.15) and the solution of (5.15), projected onto the (x, y) coordinates, is identical to the solution of (2.9). This invariance for eq. (5.15) follows from the identity

$$(5.16) \quad \frac{d}{dt}(m - m^\dagger(x, y)) = -\nabla_x m^\dagger(x, y)(m - m^\dagger(x, y)),$$

which is derived by noting that, under equation eq. (5.15),

$$\begin{aligned} \frac{d}{dt}m &= \nabla_x m^\dagger(x, y)[f_0(x) + m^\dagger(x, y)] + \nabla_y m^\dagger(x, y)g^\dagger(x, y) \\ &= \nabla_x m^\dagger(x, y)[f_0(x) + m] + \nabla_y m^\dagger(x, y)g^\dagger(x, y) \\ &\quad - \nabla_x m^\dagger(x, y)(m - m^\dagger(x, y)) \\ &= \frac{d}{dt}m^\dagger(x, y) - \nabla_x m^\dagger(x, y)(m - m^\dagger(x, y)). \end{aligned}$$

The proof of the RNN approximation property proceeds by approximating vector fields $g^\dagger(x, y), h^\dagger(x, y)$ by neural networks and introducing linear transformations of y and m to rewrite the approximate system (5.15) in the form (5.14). The effect of the approximation of the vector fields on the true solution is then propagated through the system and its effect controlled.

Remark 5.5. The need for data assimilation [Asch et al., 2016, Law et al., 2015, Reich and Cotter, 2015] to learn the initialization of recurrent neural networks may be understood as follows. Since m^\dagger is not known and y is not observed (and in particular $y(0)$ is not known) the desired initialization for (5.15), and thus also for approximations of this equation in which g^\dagger and h^\dagger are replaced by neural networks, is not known. Hence, if an RNN is trained on a particular trajectory, the initial condition that is required for accurate approximation of (2.9) from an unseen initial condition is not known. Furthermore the invariant manifold $m = m^\dagger(x, y)$ may be unstable under numerical approximation. However if some observations of the trajectory starting at the new initial condition are used, then data assimilation techniques can potentially learn the initialization for the RNN and also stabilize the invariant manifold. Ad hoc initialization methods are common practice [Haykin et al., 2007, Cho et al., 2014, Bahdanau et al., 2016, Pathak et al., 2018a], and rely on forcing the learned RNN with a short sequence of observed data to synchronize the hidden state. The success of these approaches likely rely on RNNs’ abilities to emulate data assimilators [Härter and Velho, 2012]; however, a more careful treatment of the initialization problem may enable substantial advances.

Remark 5.6. Reservoir computing is a variant on RNNs which has the advantage of leading to a quadratic optimization problem [Jaeger, 2001, Lukoševičius and Jaeger, 2009, Grigoryeva and Ortega, 2018]. Within the context of the continuous time RNN eq. (5.14) they correspond to randomizing (A, B, c) in (5.14b) and then choosing only parameter C to fit the data. To be concrete, this leads to

$$r(t) = \mathcal{G}_t(\{x(s)\}_{s=0}^t; r(0), A, B, c);$$

here \mathcal{G}_t may be viewed as a random function of the path-history of x upto time t and of the initial condition for r . Then C is determined by minimizing the quadratic function

$$\mathcal{J}_T(C) = \frac{1}{2T} \int_0^T \|\dot{x}(t) - f_0(x(t)) - Cr(t)\|^2 dt + \frac{\lambda}{2} \|C\|^2.$$

This may be viewed as a random feature approach on the Banach space \mathbf{X}_T ; the use of random features for learning of mappings between Banach spaces is studied by Nelsen and Stuart [2020]. In the specific setting described here care will be needed in choosing probability measure on (A, B, c) to ensure a well-behaved map \mathcal{G}_t ; furthermore data assimilation ideas [Asch et al., 2016, Law et al., 2015, Reich and Cotter, 2015] will be needed to learn an appropriate $r(0)$ in the prediction phase, as discussed in Remark 5.5 for RNNs.

6. NUMERICAL EXPERIMENTS

In this section, we present numerical experiments intended to test different hypotheses about the utility of hybrid mechanistic and data-driven modeling. We summarize our findings in Section 6.1. We define the overarching experimental setup in Section 6.2, then introduce our criteria for evaluating model performance in Section 6.3. In the Lorenz ’63 experiments (Section 6.4), we investigate how a simple

Markovian model error term can be recovered using discrete and continuous-time methods, and how those methods scale with the magnitude of error, data sampling rate, availability of training data, and number of learned parameters. In the Lorenz '96 Multiscale experiments (Section 6.5), we take this a step further by learning a Markovian closure term for a scale-separated system, as well as systems with less scale-separation. As expected, we find that the Markovian closure approach is highly accurate for a scale-separated regime. We also see that the Markovian closure has merit even in cases with reduced scale-separation. However, this situation would clearly benefit from learning a closure term with memory; Section 5.3 provides a theoretical underpinning for emerging work on non-Markovian closures (overviewed in Section 1.1.3). In Section 6.6, we demonstrate why non-Markovian closures must be carefully initialized and/or controlled (e.g. via data assimilation) in order to ensure their long-term stability and short-term accuracy.

6.1. Summary of Findings from Numerical Experiments.

- (1) We find that hybrid modeling has better predictive performance than purely data-driven methods in a wide range of settings (see Figures 2a and 2b): this includes scenarios where f_0 is highly accurate (but imperfect) and scenarios where f_0 is highly inaccurate (but nevertheless faithfully encodes much of the true structure for f^\dagger).
- (2) We find that hybrid modeling is more data-efficient than purely data-driven approaches (Figure 3).
- (3) We find that hybrid modeling is more parameter-efficient than purely data-driven approaches (Figure 4).
- (4) Purely data-driven discrete-time modeling can suffer from instabilities in the small timestep limit $\Delta t \ll 1$; hybrid discrete-time approaches can alleviate this issue when they are built from an integrator Ψ_0 , as this will necessarily encode the correct parametric dependence on $\Delta t \ll 1$ (Figure 5).
- (5) In order to leverage standard supervised regression techniques, continuous-time methods require good estimates of derivatives $\dot{x}(t)$ from the data. Figure 5 quantifies this estimation as a function of data sample rate.
- (6) Non-Markovian model error can be captured by Markovian terms in scale-separated cases. This is demonstrated quantitatively in Figures 6 to 8, and qualitatively in Figure 9.
- (7) Beyond the scale-separation limit: Markovian terms will fail for trajectory forecasting. However, Markovian terms may still reproduce invariant statistics in dissipative systems. This is demonstrated quantitatively in Figures 6 to 8; Figure 9 offers intuition for these findings.
- (8) Our setting reproduces discrete-time findings about hybrid models in the Markovian setting [Pathak et al., 2018b], and extends that approach to include continuous-time models and non-parametric representation of the model error m^\dagger (Figure 2b), finding similar results (1-3) to those in the Markovian discrete-time parametric setting (Figures 2a, 3 and 4).
- (9) Non-Markovian models must be carefully initialized, and indeed data assimilation may be needed, in order to ensure accuracy of invariant statistics (Figure 10), long-term stability (Figure 11), and accurate short-term predictions (Figure 12). We explain observed phenomena in terms of the properties of the desired lower-dimensional invariant manifold which is embedded within

the higher dimensional system used as the basis of approximation within an RNN.

6.2. Experimental Set-Up. In all experiments, whether using continuous- or discrete-time models, we train on noise-free trajectories from the true system, which is an ordinary differential equation. The problems we study provably have a compact global attractor and are provably (Lorenz '63) or empirically (Lorenz '96) ergodic; the invariant distribution is supported on the global attractor and captures the statistics of long-time trajectories which, by ergodicity, are independent of initial condition. The data trajectories are generated using scipy's implementation of Runge-Kutta 5(4) (via `solve_ivp`) with absolute and relative tolerances both 10^{-9} and maximum step size 10^{-4} [Dormand and Prince, 1980, Virtanen et al., 2020]. In order to obtain statistical results, we create 5 training trajectories from the true system of interest with initial conditions sampled independently from its attractor. We use the same procedure to generate short independent validation and testing trajectories—we use 7 validation trajectories and 10 testing trajectories. All plots use error bars to represent empirical estimates of the mean and standard deviation of the presented performance metric, as computed by ensembling the performance of the 5 models (one per training trajectory) over the 10 testing trajectories for a total of 70 random performance evaluations.

Each training procedure also involves an independent draw of the random feature functions as defined in (8.6). A validation step is subsequently performed to optimize the hyperparameters ω, β , as well as the regularization parameter λ . We automate this validation using Bayesian Optimization [Mockus, 1989], and find that it typically identifies good hyperparameters within 30 iterations. Given a realization of random features and an optimal λ , we obtain the minimizer C^* using the Moore-Penrose Pseudoinverse implemented in scipy (`pinv2`). This learned C^* , paired with its random feature realization, is then used to predict 10 unseen testing trajectories (it is given the true initial condition for each of these testing trajectories).

When implementing in continuous time, given high frequency but discrete-time data, two computational issues must be addressed: (i) extrapolation of the data to continuous time; (ii) discretization of the resulting integrals. The approach we adopt avoids “inverse crimes” in which favourable behaviour is observed because of agreement between the data generation mechanism (with a specific integrator) and the approximation of the objective functions [Colton and Kress, 2013, Kaipio and Somersalo, 2005, Wirgin, 2004]; see Queiruga et al. [2020] for further discussion of this issue. We interpolate the data with a spline, to obtain continuous time trajectories, and then discretize the integrals using a simple Riemann sum; this strikes a desirable balance between robustness and efficiency and avoids inverse crimes. The discrete-time approaches, however, are able to learn not only model-discrepancy, but also integrator-based discrepancies; hence, the discrete-time methods may artificially appear to outperform continuous-time approaches, when, in fact, their performances might simply be considered to be comparable.

6.3. Evaluation Criteria. Models are evaluated against the test set for their ability to predict individual trajectories, as well as invariant statistics (the invariant measure and the auto-correlation function).

Trajectory Validity Time: Given threshold $\gamma > 0$, we determine the first time t_γ at which the norm of the discrepancy between the true and approximate solutions

reaches γ :

$$t_\gamma = \operatorname{argmin}_{t \in [0, T]} \left\{ t: \|x(t) - x_m(t)\| = \gamma \overline{\|x(t)\|} \right\},$$

setting $t_\gamma = T$ if no such time exists. Here $x(t)$ is the true solution to eq. (2.2) and its learned approximate form is $x_m(t)$. We compute the normed time average $\overline{\|x(t)\|}$ once offline for a long trajectory of training data; note that it is non-zero for all non-trivially ergodic systems. In our experiments, we take $\gamma = 0.05$, which corresponds to a stringent 5% relative divergence from the true trajectory.

Invariant Distribution: To quantify errors in our reconstruction of the invariant measure, we consider the Kullback-Leibler (KL) divergence [Kullback and Leibler, 1951] between the true invariant measure μ and the invariant measure produced by our learned model μ_m . We approximate the divergence

$$d_{\text{KL}}(\mu, \mu_m) := \int_{\mathbb{R}} \log \left(\frac{d\mu}{d\mu_m} \right) d\mu$$

by integrating kernel density estimates of the measures with respect to the Lebesgue measure.

Autocorrelation: The autocorrelation function (ACF) may be computed with respect to the invariant distribution of the true model and the learned model, and compared. We approximate the ACF using the python implementation by Seabold and Perktold [2010], which uses a fast-fourier-transform to compute convolutions. We then compute the mean-squared-error between the true and approximate ACFs to represent a normalized L_2 norm of their difference.

6.4. Lorenz '63.

6.4.1. *Setting.* The Lorenz '63 system [Lorenz, 1963] is described by the following ordinary differential equation

$$(6.1) \quad \begin{aligned} \dot{u}_x &= a(u_y - u_x) \\ \dot{u}_y &= bu_x - u_y - u_x u_z \\ \dot{u}_z &= -cu_z + u_x u_y \end{aligned}$$

whose solutions are known to exhibit chaotic behavior for parameters $a = 10$, $b = 28$, $c = \frac{8}{3}$. We align these equations with our framework, starting from equation (2.1), by letting $x = (u_x, u_y, u_z)^T$ and defining $f^\dagger(x)$ to be the vector field appearing on the right-hand-side in eq. (6.1). We define a discrete solution operator Ψ^\dagger by numerical integration of f^\dagger over a fixed time window Δt corresponding to a uniform data sampling rate, so that the true system is given by eq. (2.1) in continuous-time and eq. (2.6) in discrete-time.

To simulate scenarios in which our available physics are good, but imperfect, we assume there exists additive unknown model error of form

$$m^\dagger(x) = \epsilon m_1(x)$$

with function m_1 determining the structure of model error, and scalar coefficient ϵ determining its magnitude. Recall that $f^\dagger = f_0 + m^\dagger$ and we assume f_0 is known to us. Our task is then to learn f^\dagger by learning m^\dagger and adding it to f_0 . The discrete solution operator Ψ_0 is obtained as in eq. (2.7) by numerical integration of f_0 over a fixed time window Δt .

To simplify exposition, we explicitly define m^\dagger , then let $f_0 := f^\dagger - m^\dagger$. We first consider the setting where

$$(6.2) \quad m_1(x) := \begin{bmatrix} 0 \\ bu_x \\ 0 \end{bmatrix}$$

(as in [Pathak et al., 2018b]) and modulate ϵ to control the magnitude of the error term. In this case, f_0 can be viewed as the Lorenz '63 equations with perturbed parameter $\tilde{b} = b(1 - \epsilon)$, where b is artificially decreased by 100%.

Then, we consider a more general case of heterogeneous, multi-dimensional residual error by drawing m_1 from a zero-mean Gaussian Process (GP) with a radial basis kernel (lengthscale 10). We form a map from \mathbb{R}^3 into itself by constructing three independent draws from a scalar-valued GP on \mathbb{R}^3 . The resulting function is visualized in two-dimensional projections in fig. 1.

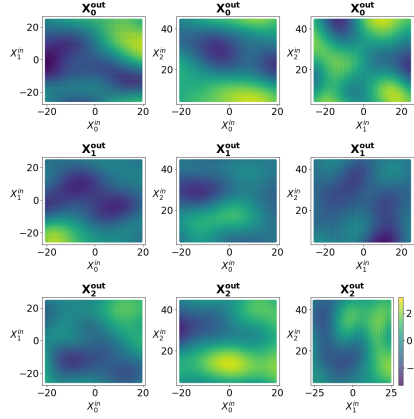


FIGURE 1. These plots show two-dimensional projections for the value of a function m_1 that represents a single random draw from a zero-mean Gaussian Process mapping $\mathbb{R}^3 \rightarrow \mathbb{R}^3$.

Observe that in the continuous-time framing, changes to ϵ do not impact the complexity of the learned error term; however, it does grow the magnitude of the error term. In the discrete-time framing, larger values of ϵ can magnify the complexity of the discrepancy $\Psi_0(x) - \Psi^\dagger(x)$.

6.4.2. Results. We perform a series of experiments with the Lorenz '63 system in order to illustrate key points about using data to learn model errors in dynamical systems. First, we demonstrate that hybrid modeling tends to outperform data-only and physics-only methods in terms of prediction quality. We first consider model error as in (6.2); see fig. 2a in which we study performance (validity time) versus model error amplitude (ϵ), using random feature maps with $D = 200$, and a single trajectory of length $T = 100$ sampled at timestep $\Delta t = 0.001$. Unless otherwise specified, this is also the configuration used in subsequent experiments.

We see identical trends in fig. 2b for a more general case with the non-parametric model error term constructed from Gaussian processes. Interestingly, we see that

for small and moderate amounts of model error ϵ , the hybrid methods substantially outperform data-only and physics-only methods. Eventually, for large enough model discrepancy, the hybrid-methods and data-only methods have similar performance; indeed the hybrid-method may be outperformed by the data-only method at large discrepancies. For the simple model error this appears to occur when the discrepancy term is larger in magnitude than f_0 (e.g. for $b = 28$ and $\epsilon = 2$, the model error term ϵbu_x can take on values larger than f^\dagger itself).

Figure 2b also shows that a continuous-time approach is favored over discrete-time when using data-only methods, but suggests the converse in the hybrid modeling context. We suspect this is an artifact of the different integration schemes used in data generation, training, and testing phases; the data are generated with a higher-fidelity integrator than the one available in training and testing. For the continuous-time method, this presents a fundamental limitation to the forecast quality (we chose this to avoid having artificially high forecast validity times). However, the discrete-time method can overcome this by not only learning the mechanistic model discrepancy, but also the discrepancy term associated with a mis-matched integrator. This typically happens when a closure is perfectly learnable and deterministic (i.e. our Lorenz '63 example); in this case, the combination of physics-based and integrator-sourced closures can be learned nearly perfectly. In later experiments with a multiscale system, the closures are considered approximate (they model the mean of a noisy underlying process) and the discrete- and continuous-time methods perform more similarly, because the inevitable imperfections of the learned closure term dominate the error rather than the mis-specified integrator. Note that approximate closures driven by scale-separation are much more realistic; thus we should not expect the hybrid discrete-time method to dramatically outperform hybrid continuous-time methods unless other limitations are present (e.g. slow sampling rate).

Importantly, the parameter regime for which hybrid methods sustain advantage over the imperfect physics-only method is substantial; the latter has trajectory predictive performance which drops off rapidly for very small ϵ . This suggests that an apparently uninformative model can be efficiently modified, by machine learning techniques, to obtain a useful model that outperforms a *de novo* learning approach.

Next, we show that hybrid methods simplify the machine learning task in terms of complexity of the learned function and, consequently, the amount of data needed for the learning. Figure 3 examines prediction performance (validity time) as a function of training data using random feature maps with $D = 2000$ and a fixed parametric model error ($\epsilon = 0.2$ in (6.2)) and sampling rate $\Delta t = 0.01$. We see that the hybrid methods substantially outperform the data-only approaches in regimes with limited training data. For the continuous-time example, we see an expected trend, where the data-only methods are able to catch up to the hybrid methods with the acquisition of more data. The discrete-time models do not exhibit this behavior, but we expect the data-only discrete-time model to eventually catch up, albeit with additional training data and number of parameters. Note that greater expressivity is also required from data-only methods—our choice of a large $D = 2000$ aims to give all methods ample expressivity, and thus test convergence with respect to training data quantity alone. These results demonstrate that the advantage of hybrid modeling is magnified when training data are limited and cannot fully inform *de novo* learning. Figure 4 further studies the impact of expressivity by again fixing

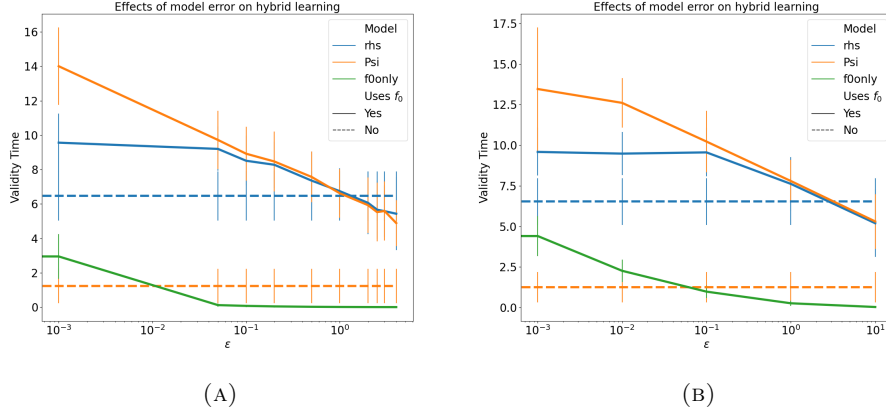


FIGURE 2. These plots show the temporal length of the forecast validity, each as a function of model error, as parameterized by ϵ . Continuous-time methods are shown in blue, discrete-time approaches in orange. Dotted lines indicate purely data-driven methods to learn the entire vector field defining the dynamics; solid lines indicate methods that learn perturbations to the imperfect mechanistic models f_0 or Ψ_0 . Integration using the imperfect mechanistic model, without recourse to data, is shown in green. (a) We reproduce qualitative results using the style of model error introduced by Pathak et al. [2018b]. (b) We extend the simulation to a residual error term governed by a Gaussian Process function shown in fig. 1. Here, we plot means, with error bars as 1 standard deviation. Both experiments were performed with $D = 200$, $T = 100$, and $\Delta t = 0.001$.

a parametric model error ($\epsilon = 0.05$ in (6.2)), training length $T = 100$, and sampling rate $\Delta t = 0.001$. We see that all methods improve with a larger number of random features, but that relative superiority of hybrid methods is maintained even for $D = 10000$.

Finally, we study trade-offs between learning in discrete- versus continuous-time. Figure 5 examines prediction performance (validity time) as a function of data sampling rate Δt using random feature maps with $D = 200$ with a fixed parametric model error ($\epsilon = 0.05$ in (6.2)) and an abundance of training data $T = 1000$. We observe that for fast sampling rates ($\Delta t < 0.01$), the continuous-time and discrete-time hybrid methods have similar performance. For $\Delta t > 0.01$, derivatives become difficult to estimate from the data and the performance of the continuous-time methods rapidly decline. However, the discrete-time methods sustain their predictive performance for slower sampling rates ($\Delta t \in (0.01, 0.1)$). At some point, the discrete-time methods deteriorate as well, as the discrete map becomes complex to learn at longer terms because of the sensitivity to initial conditions that is a hallmark of chaotic systems. Here, the discrete-time methods begin to fail around $\Delta t = 0.2$; note that they can be extended to longer time intervals by increasing D and amount of training data, but the returns diminish quickly.

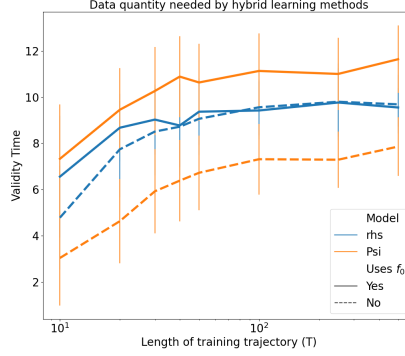


FIGURE 3. Here we examine the performance of the proposed methods as a function of training data, where $\Delta t = 0.01$, ($\epsilon = 0.2$ in (6.2)), and $D = 2000$ are held constant. Continuous-time methods are shown in blue and discrete-time approaches in orange. Dotted lines indicate purely data-driven methods and solid lines indicate methods that learn perturbation to the imperfect mechanistic models f_0 or Ψ_0 . We observe that all methods improve with increasing training lengths. We see that, in continuous-time, the primary benefit in hybrid modeling is when the training data are limited in volume

6.5. Lorenz '96 Multiscale System.

6.5.1. *Setting.* Here, we consider the multiscale system [Lorenz, 1996] of form (2.8), where each variable $X_k \in \mathbb{R}$ is coupled to a subgroup of fast variables $Y_k \in \mathbb{R}^J$. We have $X \in \mathbb{R}^K$ and $Y \in \mathbb{R}^{K \times J}$. For $k = 1 \dots K$ and $j = 1 \dots J$, we write

$$(6.3a) \quad \dot{X}_k = f_k(X) + h_x \bar{Y}_k$$

$$(6.3b) \quad \dot{Y}_{k,j} = \frac{1}{\varepsilon} r_j(X_k, Y_k)$$

$$(6.3c) \quad \bar{Y}_k = \frac{1}{J} \sum_{j=1}^J Y_{k,j}$$

$$(6.3d) \quad f_k(X) = -X_{k-1}(X_{k-2} - X_{k+1}) - X_k + F$$

$$(6.3e) \quad r_j(X_k, Y_k) = -Y_{k,j+1}(Y_{k,j+2} - Y_{k,j-1}) - Y_{k,j} + h_y X_k$$

$$(6.3f) \quad X_{k+K} = X_k, \quad Y_{k+K,j} = Y_{k,j}, \quad Y_{k,j+J} = Y_{k+1,j}$$

where $\varepsilon > 0$ is a scale-separation parameter, $h_x, h_y \in \mathbb{R}$ govern the couplings between the fast and slow systems, and $F > 0$ provides a constant forcing. We set $K = 9$, $J = 8$, $h_x = -0.8$, $h_y = 1$, $F = 10$; this leads to chaotic dynamics for ε small. When studying scale-separation, we consider $\varepsilon \in \{2^{-7}, 2^{-5}, 2^{-3}, 2^{-1}\}$.

We consider the setting in which we try to learn Markovian models in variable X alone, from X data generated by the coupled (X, Y) system. Large scale-separation between the observed (X) and unobserved (Y) spaces can simplify the problem

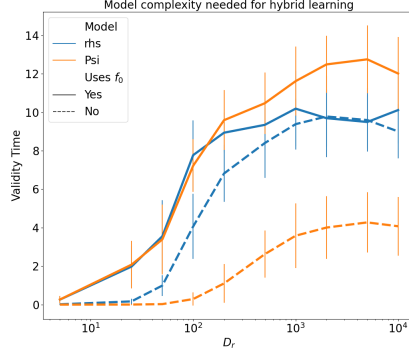


FIGURE 4. Here we examine the performance of the proposed methods as a function of model complexity, where $\Delta t = 0.001$, $\epsilon = 0.05$, and $T = 100$ are held constant. Continuous-time methods are shown in blue and discrete-time approaches in orange. Dotted lines indicate purely data-driven methods and solid lines indicate methods that use the mechanistic models f_0 or Ψ_0 . We observe that all methods improve with increasing number of parameters, and that hybrid methods are especially beneficial when available complexity is limited.

of accounting for the unobserved components; in particular, for sufficient scale-separation, we expect a Markovian term to recover a large majority of the residual errors. In fact, we further simplify this problem by learning a scalar-valued model error M that is applied to each X_k identically in the slow system:

$$\dot{X}_k \approx f_k(X) + M(X_k).$$

This choice stems from observations about statistical interchangeability amongst the slow variables of the system; these properties of the Lorenz '96 Multiscale model in the scale-separated regime are discussed in [Fatkullin and Vanden-Eijnden, 2004]. We can directly align our reduction of eq. (6.3) with the Markovian hybrid learning framework in eq. (2.2) as follows:

$$\begin{aligned} \dot{X} &\approx f_0(X) + m(X) \\ f_0(X) &:= [f_1(X), \dots, f_K(X)]^T \\ m(X) &:= [M(X_1), \dots, M(X_K)]^T. \end{aligned}$$

6.5.2. Results. We plot the performance gains of our hybrid learning approaches in fig. 6 by considering validity times of trajectory forecasts, estimation of the invariant measure, and estimation of the autocorrelation function. In all three metrics (and for all scale-separations ϵ), *de novo* learning in discrete ($\Psi^\dagger \approx m$) and continuous-time ($f^\dagger \approx m$) is inferior to using the nominal mechanistic model f_0 . We found that the amount of data used in these experiments is insufficient to learn the full system from scratch. On the other hand, hybrid models in discrete ($\Psi^\dagger \approx \Psi_0 + m$) and continuous-time ($f^\dagger \approx f_0 + m$) noticeably outperformed the nominal physics.

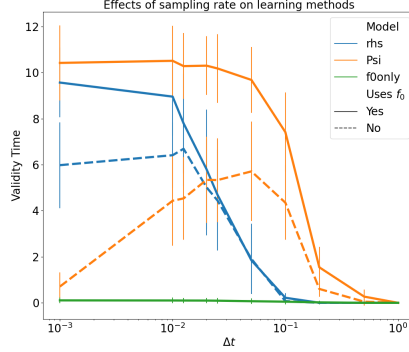


FIGURE 5. This shows temporal forecast validity as a function of the step size of training data for the tested methods. We hold fixed $D = 200$, $\epsilon = 0.05$, and $T = 1000$. Continuous-time methods are shown in blue, discrete-time approaches in orange, and physics-only methods in green. Dotted lines indicate purely data-driven methods and solid lines indicate methods that use the mechanistic models f_0 or Ψ_0 . We see that while purely data-driven discrete-time methods struggle at short time steps, the hybrid version thrives in this scenario. All approaches, of course, eventually decay as the large time steps create more complex forward maps, because of sensitivity to initial conditions. We also see that continuous-time methods work very well for small time steps, then deteriorate in tandem with the quality of our estimated derivatives.

Surprisingly, fig. 6 shows that the Markovian closure methods still qualitatively reproduce the invariant statistics even for large ϵ settings where we would expect substantial memory effects. Figures 7 and 8 demonstrate this quantitatively using KL-divergence between invariant measures and mean-squared-error between auto-correlation functions. It seems that for this dissipative system, memory effects tend to average out in the invariant statistics. However, the improvements in validity time for trajectory-based forecasting deteriorate for $\epsilon = 2^{-1}$.

To visualize this non-Markovian structure, and how it might be exploited, we examine the residuals from f_0 in fig. 9 and observe that there are discernible trajectories walking around the Markovian closure term. For small ϵ , these trajectories oscillate rapidly around the closure term. For large ϵ (e.g. 2^{-1}), however, we observe a slow-moving residual trajectory around the Markovian closure term. This indicates the presence of a stronger memory component, and thus would benefit from a non-Markovian approach to closure modeling.

6.6. Initializing and Stabilizing the RNN. As mentioned in Remark 5.5 the RNN approximates an enlarged system which contains solutions of the original system as trajectories confined to the invariant manifold $m = m^\dagger(x, y)$; see identity (5.16). However, this invariant manifold may be unstable, either as a manifold within the continuous time model (5.15), or as a result of numerical instability. We now demonstrate this with numerical experiments. This instability points to the

need for data assimilation to be used with RNNs if prediction of the original system is desired, not only to initialize the system but also to stabilize the dynamics to remain near to the desired invariant manifold.

To illustrate these challenges, we consider the problem of modeling evolution of a single component of the Lorenz '63 system eq. (6.1). Consider this as variable x in eq. (2.8). As exhibited in eq. (5.15), model error may be addressed in this setting by learning a representation that contains the hidden states y in eq. (2.8) (i.e. the other two unobserved components of eq. (6.1)), but since the dimension of the hidden states is typically not known *a priori* the dimensions of the latent variables in the RNN (and the system it approximates) may be greater than those of y ; in the specific construction we use to prove the existence of an approximating RNN we introduce a vector field for evolution of the error m as well as y . We now discuss the implications of embedding the true dynamics in a higher dimensional system in the specific context of the embedded system eq. (5.15). However the observations apply to any embedding of the desired dynamics (2.8) (with $\epsilon = 1$) within any higher dimensional system.

We choose examples for which eq. (5.16) implies that $m - m^\dagger$ is constant in time. Then, under eq. (5.15),

$$(m - m^\dagger(x, y))(t) = \text{constant};$$

that is, it is constant in time. The desired invariant manifold (where the constant is 0) is thus stable. However this stability only holds in a neutral sense: linearization about the manifold exhibits a zero eigenvalue related to translation of $m - m^\dagger$ by a constant. We now illustrate that this embedded invariant manifold can be unstable; in this case the instability is caused by numerical integration, which breaks the conservation of $m - m^\dagger$ in time.

Example 1: Consider equation eq. (6.1) which we write in form eq. (2.9) by setting $x = u_x$ and $y = (u_y, u_z)$. Then we let $f_0(u_x) := -au_x$ yielding $m^\dagger(u_y) = au_y$. Thus $f^\dagger = f_0 + m^\dagger$ is defined by the first component of the right-hand side of eq. (6.1). The function $g^\dagger(u_y, u_z)$ is then given by the second and third components of the right-hand side of eq. (6.1). Applying the methodology leading to eq. (5.15) to eq. (6.1) results in the following four dimensional system:

$$(6.4a) \quad \dot{u}_x = f_0(u_x) + m, \quad u_x(0) = x_0,$$

$$(6.4b) \quad \dot{u}_y = bu_x - u_y - u_x u_z, \quad u_y(0) = y_0,$$

$$(6.4c) \quad \dot{u}_z = -cu_z + u_x u_y, \quad u_z(0) = z_0,$$

$$(6.4d) \quad \dot{m} = a(bu_x - u_y - u_x u_z), \quad m(0) = m^\dagger(y_0).$$

Here we have omitted the u_y -dependence from the equation (6.1) for u_x , and aim to learn this error term; we introduce the variable m in order to do so. This system, when projected into u_x, u_y, u_z , behaves identically to eq. (6.1) when $m(0) = m^\dagger(y_0)$. Thus the 4-dimensional system in eq. (6.4) has an embedded invariant manifold on which the dynamics is coincident with that of the 3-dimensional Lorenz '63 system.

We numerically integrate the 4-dimensional system in eq. (6.4) for 10000 model time units (initialized at $x_0 = 1, y_0 = 3, z_0 = 1, m_0 = ay_0 = 30$), and show in Figure 10 that the resulting measure for u_x (dashed red) is nearly identical to its invariant measure in the traditional 3-dimensional Lorenz '63 system in eq. (6.1) (solid black). However, we re-run the simulation for a perturbed $m(0) = m^\dagger(y_0) + 1$, and see in Figure 10 (dotted blue) that this yields a different invariant measure for

u_x . This result emphasizes the importance of correctly initializing an RNN not only for efficient trajectory forecasting, but also for accurate statistical representation of long-time behavior.

Example 2: Now we consider eq. (6.1) which we write in form eq. (2.9) by setting $x = u_z$ and $y = (u_x, u_y)$. We let $f_0(u_z) := -cu_z$ and $m^\dagger(u_x, u_y) := u_x u_y$, so that $f^\dagger = f_0 + m^\dagger$ corresponds to the third component of the right-hand side of eq. (6.1). Function $g^\dagger(u_x, u_y)$ is defined by the first two components of the right-hand side of eq. (6.1). We again form a 4-dimensional system corresponding to eq. (6.1) using the methodology that leads to eq. (5.15):

$$\begin{aligned}
 (6.5a) \quad & \dot{u}_x = a(u_y - u_x), & u_x(0) &= x_0, \\
 (6.5b) \quad & \dot{u}_y = bu_x - u_y - u_x u_z, & u_y(0) &= y_0, \\
 (6.5c) \quad & \dot{u}_z = f_0(u_z) + m, & u_z(0) &= z_0, \\
 (6.5d) \quad & \dot{m} = u_x \dot{u}_y + u_y \dot{u}_x, & m(0) &= m^\dagger(x_0, y_0).
 \end{aligned}$$

We integrate eq. (6.5) for 3000 model time units (initialized at $x_0 = 1, y_0 = 3, z_0 = 1, m_0 = x_0 y_0 = 3$), and show in Figure 11 that the 3-dimensional Lorenz attractor is unstable with respect to perturbations in the numerical integration of the 4-dimensional system. The solutions for u_x, u_y, u_z eventually collapse to a fixed point after the growing discrepancy between $m(t)$ and m^\dagger becomes too large. The time at which collapse occurs may be delayed by using smaller tolerances within the numerical integrator (we employ MATLAB RK45) demonstrating that the instability is caused by the numerical integrator. This collapse is very undesirable if prediction of long-time statistics is a desirable goal. On the other hand, Figure 12 shows short-term accuracy of the 4-dimensional system in eq. (6.5) up to 12 model time units when correctly initialized ($m_0 = m^\dagger(x_0, y_0)$, dashed red), and accuracy up to 8 model time units when initialization of m_0 is perturbed ($m_0 = m^\dagger(x_0, y_0) + 1$, dotted blue). This result demonstrates the fundamental challenges of representing chaotic attractors in enlarged dimensions, and may help explain observations of RNNs yielding good short-term accuracy, but inaccurate long-term statistical behavior.

7. CONCLUSIONS

In this work we evaluate the utility of blending mechanistic models of dynamical systems with data-driven methods, demonstrating the power of hybrid approaches. We provide a mathematical framework that is consistent across parametric and non-parametric models, encompasses both continuous- and discrete-time, and allows for Markovian and memory-dependent model error. We also provide basic theoretical results that underpin the adopted approaches. The unified framework elucidates commonalities between seemingly disparate approaches across various applied and theoretical disciplines. It would be desirable if the growing recognition of the need for hybrid modeling were to motivate flexible incorporation of mechanistic models into open-source software for continuous-time Markovian and non-Markovian modeling of error [Rubanova et al., 2019, Chang et al., 2019, Erichson et al., 2020, Anantharaman et al., 2020, Gupta and Lermusiaux, 2021].

Our examples of introducing artificial model error into the Lorenz '63 system demonstrate the superiority of hybrid modeling over learning an entire system from scratch, even when the available mechanistic model has large infidelities. Hybrid modeling also showed surprisingly large performance gains over using mechanistic

models with only small infidelities. We quantify these improvements in terms of data hunger, demands for model complexity, and overall predictive performance, and find that all three are significantly improved by hybrid methods in our experiments.

We establish bounds on the excess risk and generalization error that decay as $1/\sqrt{T}$ when learning model discrepancy from a trajectory of length T in an ergodic continuous-time Markovian setting. We make minimal assumptions about the nominal physics (i.e. $f_0 \in C^1$); thus, our result equivalently holds for learning the entire vector field f^\dagger (i.e. $f_0 \equiv 0$). However the upper bounds on excess risk and generalization error scale with the size of the function being learned, hence going some way towards explaining the superiority of hybrid modeling observed in the numerical experiments. Future theoretical work aimed at quantifying the benefits of hybrid learning versus purely data-driven learning is of interest. We also note that the ergodic assumption underlying our theory will not be satisfied by many dynamical models, and alternate statistical learning theories need to be developed in such settings.

We illustrate trade-offs between discrete-time and continuous-time modeling approaches by studying their performance as a function of training data sample rate. In the Lorenz '63 experiments, we find that hybrid discrete-time approaches can alleviate instabilities seen in purely data-driven discrete-time models at small timesteps; this is likely due to structure of integrator Ψ_0 , which has the correct parametric dependence on timestep. In the continuous-time setting, we find that performance is best when derivatives can accurately be reconstructed from the data, and deteriorates in tandem with differentiation inaccuracies (caused by large timesteps); continuous-time hybrid methods appear to offer additional robustness to inaccurate differentiation when compared to purely data-driven methods. In cases of large timesteps and poorly resolved derivatives, ensemble-based data assimilation methods may still allow for accurate learning of residuals to the flow field for continuous-time modeling [Gottwald and Reich, 2021].

Finally, we study non-Markovian memory-dependent model error within the context of the Lorenz '96 Multiscale system. We find that, while Markovian closure approaches succeed in modeling invariant statistics under various degrees of scale-separation, trajectory forecast quality decreases with scale-separation. To address challenges of non-Markovian hybrid modeling, we prove universal approximation for continuous-time hybrid RNNs. Future work focusing on implementation of these approaches, and reservoir computing variants, would be of interest. This work on RNNs and reservoir computing will need to focus on the data assimilation problem of learning the initialization of the latent variable; in addition, these methods will benefit from constraining the learning to ensure stability of the latent dynamical model. These issues are illustrated via numerical experiments that relate RNNs to the question of stability of invariant manifolds representing embedded desired dynamics within a higher dimensional system.

8. APPENDIX

8.1. Proof of Excess Risk/Generalization Error Theorem. In the following we may assume, without loss of generality, that the functions $\{f_\ell\}_{\ell=0}^p$ and m^\dagger are bounded on \mathbb{R}^{d_x} ; this is because they are only evaluated along trajectories that live on the global attractor \mathcal{A} , which is bounded; they may hence be smoothly modified outside \mathcal{A} without changing the analysis.

Lemma 8.1. *Let Assumptions A1 and A2 hold. Then there is Σ positive semi-definite symmetric in $\mathbb{R}^{p \times p}$ such that $\theta_T^* \rightarrow \theta_\infty^*$ almost surely, and $\sqrt{T}(\theta_T^* - \theta_\infty^*) \Rightarrow N(0, \Sigma)$ with respect to $x(0) \sim \mu$. Furthermore, there is constant $C \in (0, \infty)$ such that, almost surely w.r.t. $x(0) \sim \mu$,*

$$\limsup_{T \rightarrow \infty} \left(\frac{T}{\log \log T} \right)^{\frac{1}{2}} \|\theta_T^* - \theta_\infty^*\| \leq C.$$

Proof. By rearranging the equation for θ_∞^* we see that

$$\begin{aligned} A_T \theta_T^* &= b_T, \\ A_T \theta_\infty^* &= b_\infty + (A_T - A_\infty) \theta_\infty^*. \end{aligned}$$

Thus, subtracting,

$$(8.1) \quad (\theta_T^* - \theta_\infty^*) = A_T^{-1}(b_T - b_\infty) - A_T^{-1}(A_T - A_\infty)\theta_\infty^*.$$

Because $\{f_\ell(\cdot)\}$ and $m^\dagger(\cdot)$ are Hölder and bounded (Assumption A2), so are $\langle f_i(\cdot), f_j(\cdot) \rangle$ and $\langle m^\dagger(\cdot), f_j(\cdot) \rangle$. Thus each entry of matrix A_T (resp. vector b_T) converges almost surely to its corresponding entry in A_∞ (resp. b_∞), by Assumption A1. The almost sure convergence of θ_T^* to θ_∞^* follows, after noting that A_∞ is invertible. Furthermore, also by Assumption A1, there are constants $\{\sigma_{ij}\}, \{\sigma_j\}$ such that

$$\begin{aligned} \sqrt{T} \left((A_T)_{ij} - (A_\infty)_{ij} \right) &\Rightarrow N(0, \sigma_{ij}^2), \\ \sqrt{T} \left((b_T)_j - (b_\infty)_j \right) &\Rightarrow N(0, \sigma_j^2). \end{aligned}$$

Since arbitrary linear combinations of the $\{(A_T)_{ij}\}, \{(b_T)_j\}$ are time-averages of Hölder functions, it follows that $\{A_T - A_\infty, b_T - b_\infty\}$ converges in distribution to a Gaussian, at rate $1/\sqrt{T}$ by the Cramér-Wold Theorem [Grimmett and Stirzaker, 2020]. Weak convergence of $\theta_T^* - \theta_\infty^*$ to a Gaussian, at rate $1/\sqrt{T}$, follows from (8.1) by use of the Slutsky Lemma [Grimmett and Stirzaker, 2020], since A_T converges almost surely to invertible A_∞ . Matrix Σ cannot be identified explicitly in terms of only the $\{\sigma_{ij}\}, \{\sigma_i\}$ because of correlations between A_T and b_T . The almost sure bound on $\|\theta_T^* - \theta_\infty^*\|$ follows from (8.1) after multiplying by $(T/\log \log T)^{\frac{1}{2}}$, noting that $A_T \rightarrow A_\infty$ almost surely, and the almost sure bounds on $(T/\log \log T)^{\frac{1}{2}} \{\|A_T - A_\infty\|, \|b_T - b_\infty\|\}$, using Assumption A1. \square

In what follows it is helpful to define

$$\begin{aligned} R^+ &= (\theta_T^* - \theta_\infty^*)(\|\theta_T^*\| + \|\theta_\infty^*\| + 1), \\ G^+ &= \mathcal{I}_T(m_\infty^*) - \mathcal{I}_\infty(m_\infty^*). \end{aligned}$$

Lemma 8.2. *Let Assumption A2 hold. Then there is constant $C > 0$ such that the excess risk R satisfies*

$$R \leq C\|R^+\|$$

Furthermore the generalization error satisfies

$$|G| \leq 2C\|R^+\| + |G^+|.$$

Proof. For the bound on the excess risk we note that

$$\begin{aligned} R &= \mathcal{L}_\mu(m_T^*, m^\dagger) - \mathcal{L}_\mu(m_\infty^*, m^\dagger) = \int_{\mathbb{R}^{d_x}} \left\langle (m_T^* - m_\infty^*)(x), (m_T^* + m_\infty^* - 2m^\dagger)(x) \right\rangle \mu(dx) \\ &\leq \left(\int_{\mathbb{R}^{d_x}} \|(m_T^* - m_\infty^*)(x)\|^2 \mu(dx) \right)^{\frac{1}{2}} \left(\int_{\mathbb{R}^{d_x}} \|(m_T^* + m_\infty^* - 2m^\dagger)(x)\|^2 \mu(dx) \right)^{\frac{1}{2}}. \end{aligned}$$

The first follows from the boundedness of the $\{f_\ell\}_{\ell=1}^p$ and m^\dagger , since the first term in the product above is bounded by a constant multiple of $\|\theta_T^* - \theta_\infty^*\|$ and the second term by a constant multiple of $\|\theta_T^*\| + \|\theta_\infty^*\| + \sup \|m^\dagger\|$.

For the bound on the generalization error we note that

$$\begin{aligned} G &= \mathcal{I}_T(m_T^*) - \mathcal{I}_\infty(m_T^*) \\ &= \mathcal{I}_T(m_T^*) - \mathcal{I}_T(m_\infty^*) \\ &\quad + \mathcal{I}_T(m_\infty^*) - \mathcal{I}_\infty(m_\infty^*) \\ &\quad + \mathcal{I}_\infty(m_\infty^*) - \mathcal{I}_\infty(m_T^*) \\ &= (\mathcal{I}_T(m_T^*) - \mathcal{I}_T(m_\infty^*)) + G^+ - R. \end{aligned}$$

The third term in the final identity is the excess risk that we have just bounded; the first term may be bounded in the same manner that we bounded the excess risk, noting that integration with respect to μ is simply replaced by integration with respect to the empirical measure generated by the trajectory data; the second term is simply G^+ . Thus the result follows. \square

Proof of Theorem 5.2. By Assumption A1, with choice of $\varphi(x) = \|m^\dagger(x) - m_\infty^*(x)\|^2$, $\sqrt{T}G^+$ converges in distribution to a scalar-valued centred Gaussian. By Lemma 8.1 and the Slutsky Lemma [Grimmett and Stirzaker, 2020], $\sqrt{T}R^+$ converges in distribution to a centred Gaussian in \mathbb{R}^p . By the Cramer-Wold Theorem [Grimmett and Stirzaker, 2020] $\sqrt{T}(R^+, G^+)$ converges in distribution to a centred Gaussian in \mathbb{R}^{p+1} .

The convergence in distribution results for excess risk R and generalization error $|G|$ then follow from Lemma 8.2, under Assumption A1. Furthermore, by Lemma 8.1, there is constant $C_1 > 0$ such that

$$\limsup_{T \rightarrow \infty} \left(\frac{T}{\log \log T} \right)^{\frac{1}{2}} \|R^+\| \leq C_1;$$

similarly, possibly by enlarging C_1 , Assumption A1 gives

$$\limsup_{T \rightarrow \infty} \left(\frac{T}{\log \log T} \right)^{\frac{1}{2}} |G^+| \leq C_1.$$

The desired almost sure bound on $R + |G|$ follows from Lemma 8.2. \square

8.2. Proof of Continuous-Time RNN Approximation Theorem.

Proof. Recall equations (5.15). By approximation theory by means of two-layer feed-forward neural networks [Cybenko, 1989], for any $\delta_o > 0$ there exist embedding dimensions N_g and N_h and parameterizations

$$\begin{aligned} \theta_g &= \{A_g \in \mathbb{R}^{d_y \times N_g}, B_g \in \mathbb{R}^{N_g \times d_x}, C_g \in \mathbb{R}^{N_g \times d_y}, c_g \in \mathbb{R}^{N_g}\}, \\ \theta_h &= \{A_h \in \mathbb{R}^{d_x \times N_h}, B_h \in \mathbb{R}^{N_h \times d_x}, C_H \in \mathbb{R}^{N_h \times d_y}, c_h \in \mathbb{R}^{N_h}\} \end{aligned}$$

such that for any $(x, y) \in B(0, 2\rho_T)$

$$\begin{aligned}\|g^\dagger(x, y) - A_g\sigma(B_gx + C_gy + c_g)\| &\leq \delta_o \\ \|h^\dagger(x, y) - A_h\sigma(B_hx + C_hy + c_h)\| &\leq \delta_o.\end{aligned}$$

Without loss of generality we may assume that A_g and A_h have full rank since, if they do not, arbitrarily small changes can be made which restore full rank. By using these parameterizations and embedding dimensions, we can rewrite eq. (5.15) as

$$\begin{aligned}(8.2) \quad \dot{x} &= f_0(x) + m \\ \dot{y} &= A_g\sigma(B_gx + C_gy + c_g) + e_y(t) \\ \dot{m} &= A_h\sigma(B_hx + C_hy + c_h) + e_{m^\dagger}(t)\end{aligned}$$

where, uniformly for $(x(0), y(0)) \in B(0, \rho_0)$,

$$\begin{aligned}\sup_{t \in [0, T]} \|e_y(t)\| &\leq \delta_o \\ \sup_{t \in [0, T]} \|e_{m^\dagger}(t)\| &\leq \delta_o.\end{aligned}$$

By removing the bounded error terms, we obtain the following approximate system:

$$\begin{aligned}(8.3) \quad \dot{x}_\delta &= f_0(x_\delta) + m_\delta \\ \dot{y}_\delta &= A_g\sigma(B_gx_\delta + C_gy_\delta + c_g) \\ \dot{m}_\delta &= A_h\sigma(B_hx_\delta + C_hy_\delta + c_h)\end{aligned}$$

Here $m_\delta(t)$ is initialized at $m^\dagger(x(0), y(0))$.

Next, we obtain a stability bound on the discrepancy between the approximate system eq. (8.3) and the true system (originally written as eq. (2.9) and re-formulated as eq. (8.2)). First, let $w = (x, y, m)$, $w_\delta = (x_\delta, y_\delta, m_\delta)$ and define F to be the concatenated right-hand-side of eq. (8.3). Note that F is L -Lipschitz for some L related to the Lipschitz continuity of f_0 , approximation parameterization θ_δ , and regularity of nonlinear activation function σ . Then we can write the true and approximate systems, respectively, as

$$(8.4a) \quad \dot{w} = F(w) + e_w(t)$$

$$(8.4b) \quad \dot{w}_\delta = F(w_\delta),$$

where

$$\sup_{t \in [0, T]} \|e_w(t)\| \leq \sup_{t \in [0, T]} \|e_y(t)\| + \sup_{t \in [0, T]} \|e_{m^\dagger}(t)\| \leq 2\delta_o.$$

Let $Pw = (x, y)$ and $P^\perp w = m$; recall that $P^\perp w(0)$ is defined in terms of $Pw(0)$. Then, for any $t \in [0, T]$, and for all $Pw(0), Pw_\delta(0) \in B(0, \rho_0)$

$$\|w(t) - w_\delta(t)\| \leq \|w(0) - w_\delta(0)\| + \int_0^t \|e_w(s)\| ds + \int_0^t \|F(w(s)) - F(w_\delta(s))\| ds.$$

This follows by writing eq. (8.4) in integrated form, subtracting and taking norms. Using the facts that $\|e_w(s)\| \leq 2\delta_o$ and F is L -Lipschitz we obtain, for $t \in [0, T]$,

$$\|w(t) - w_\delta(t)\| \leq \|w(0) - w_\delta(0)\| + 2\delta_o T + L \int_0^t \|w(s) - w_\delta(s)\| ds.$$

By the integral form of the Gronwall Lemma, it follows that for all $t \in [0, T]$:

$$\|w(t) - w_\delta(t)\| \leq [\|w(0) - w_\delta(0)\| + 2\delta_o T] \exp(Lt).$$

Thus,

$$\sup_{t \in [0, T]} \|w(t) - w_\delta(t)\| \leq [\|w(0) - w_\delta(0)\| + 2\delta_o T] \exp(LT).$$

By choice of initial conditions and δ_o sufficiently small we can achieve a $\delta > 0$ approximation.

Finally, we note that the approximate system eq. (8.3) may be written as a recurrent neural network of form eq. (5.14) as follows. Consider the equations

$$\begin{aligned} \dot{x}_\delta &= f_0(x_\delta) + A_h n_\delta \\ \dot{z}_\delta &= \sigma(B_g x_\delta + C_g A_g z_\delta + c_g) \\ \dot{n}_\delta &= \sigma(B_h x_\delta + C_h A_g z_\delta + c_h) \end{aligned} \tag{8.5}$$

and notice that $y_\delta = A_g z_\delta$ and $m_\delta = A_h n_\delta$. Now note that eq. (8.5) is equivalent to eq. (5.14), with recurrent state r_δ and parameters θ_δ given by:

$$\begin{aligned} \bullet \quad r_\delta &= \begin{bmatrix} z_\delta \\ n_\delta \end{bmatrix} \\ \bullet \quad A_\delta &= \begin{bmatrix} 0 & A_h \end{bmatrix} \\ \bullet \quad B_\delta &= \begin{bmatrix} B_g \\ B_h \end{bmatrix} \\ \bullet \quad C_\delta &= \begin{bmatrix} C_g A_g & 0 \\ C_h A_g & 0 \end{bmatrix} \\ \bullet \quad c_\delta &= \begin{bmatrix} c_g \\ c_h \end{bmatrix} \end{aligned}$$

Any initial condition on $(y_\delta(0), m_\delta(0))$ may be achieved by choice of initializations for $(z_\delta(0), n_\delta(0))$, since A_g, A_h are of full rank. □

8.3. Random Feature Approximation. Random feature methods lead to function approximation for mappings between Hilbert spaces $X \rightarrow Y$. They operate by constructing a probability space $(\Theta, \nu, \mathcal{F})$ with $\Theta \subseteq \mathbb{R}^p$ and feature map $\varphi: X \times \Theta \rightarrow Y$ such that $k(x, x') := \mathbb{E}^\vartheta[\varphi(x; \vartheta) \otimes \varphi(x'; \vartheta)] \in \mathcal{L}(Y, Y)$ forms a reproducing kernel in an associated reproducing kernel Hilbert space (RKHS) K . Solutions are sought within $\text{span}\{\varphi(\cdot; \vartheta_l)\}_{l=1}^m$ where the $\{\vartheta_l\}$ are picked i.i.d. at random. Theory supporting the approach was established in finite dimensions by Rahimi and Recht [2008a]; the method was recently applied in the infinite dimensional setting in [Nelsen and Stuart, 2020].

We now explain the precise random features setting adopted in Section 5, and hypothesis classes given by (5.1) and (5.2). We start with random feature functions

$\varphi(\cdot; \vartheta): \mathbb{R}^{d_x} \rightarrow \mathbb{R}$, with $\vartheta = [w, b]$,

$$(8.6) \quad \begin{aligned} w &\in \mathbb{R}^{d_x} \sim \mathcal{U}(-\omega, \omega) \\ b &\in \mathbb{R} \sim \mathcal{U}(-\beta, \beta) \\ \varphi(x; w, b) &:= \tanh(w^T x + b), \end{aligned}$$

and $\omega, \beta > 0$. We choose D i.i.d. draws of w, b , and stack the resulting random feature functions to form the map $\phi(x): \mathbb{R}^{d_x} \rightarrow \mathbb{R}^D$ given by

$$\phi(x) := [\varphi(x; w_1, b_1) \quad \dots \quad \varphi(x; w_D, b_D)]^T.$$

We define hypothesis class (5.1) by introducing matrix $C: \mathbb{R}^D \rightarrow \mathbb{R}^{d_x}$ and seeking approximation to model error in the form $m(x) = C\phi(x)$ by optimizing a least squares function over matrix C . This does not quite correspond to the random features model with $X = Y = \mathbb{R}^{d_x}$ because, when written as a linear span of vector fields mapping \mathbb{R}^{d_x} into itself, the vector fields are not independent. Nonetheless we have found this approach convenient in practice and employ it in our numerical experiments.

To align with the random features model with $X = Y = \mathbb{R}^{d_x}$, we may choose $D = d_x$ and then draw p functions $\phi(\cdot)$, labelled as $\{f_\ell(\cdot)\}$ i.i.d. at random from the preceding construction, leading to hypothesis class (5.2): we then seek approximation to model error in the form $m(x) = \sum_{\ell=1}^p \theta_\ell f_\ell(x)$. We find this form of random features model the most convenient to explain the learning theory perspective on model error.

8.4. Derivation of Tikhonov-Regularized Linear Inverse Problem. Here, we show that optimization of eq. (5.3)

$$\mathcal{J}_T(C) = \frac{1}{2T} \int_0^T \|\dot{x}(t) - f_0(x) - C\phi(x(t))\|^2 dt + \frac{\lambda}{2} \|C\|^2$$

reduces to a Tikhonov-regularized linear inverse problem. Since eq. (5.6) is quadratic in C , there exists a unique global minimizer for C^* such that $\frac{\partial \mathcal{J}_T}{\partial C}(C^*) = 0$. The minimizer C^* satisfies:

$$(Z + \lambda I)C^T = Y$$

where

$$\begin{aligned} Z &= \overline{[\phi \otimes \phi]}_T \\ Y &= \overline{[\phi \otimes (\dot{x} - f_0)]}_T. \end{aligned}$$

and

$$[A \otimes B]_t := A(t)B^T(t)$$

$$\overline{A}_T := \frac{1}{T} \int_0^T A(t) dt$$

for $A(t) \in \mathbb{R}^{m \times n}$, $B(t) \in \mathbb{R}^{m \times l}$.

To see this, observe that

$$\begin{aligned}
\mathcal{J}_T(C) &= \frac{1}{2T} \int_0^T \|\dot{x}(t) - f_0(x(t)) - C\phi(x(t))\|^2 dt + \frac{\lambda}{2} \|C\|^2 \\
&= \frac{1}{2T} \int_0^T \|\dot{x}(t) - f_0(x(t))\|^2, \\
&\quad + \langle C\phi(x(t)), C\phi(x(t)) \rangle - 2\langle \dot{x}(t) - f_0(x(t)), C\phi(x(t)) \rangle dt + \frac{\lambda}{2} \langle C, C \rangle
\end{aligned}$$

and

$$\frac{\partial \mathcal{J}_T(C)}{\partial C} = \frac{1}{2T} \int_0^T 2C[\phi(x(t)) \otimes \phi(x(t))] - 2[(\dot{x}(t) - f_0(x(t))) \otimes \phi(x(t))] dt + \lambda C.$$

By setting the gradient to zero, we see that

$$C \left[\frac{1}{T} \int_0^T [\phi(x(t)) \otimes \phi(x(t))] dt + \lambda I \right] = \frac{1}{T} \int_0^T [(\dot{x}(t) - f_0(x(t))) \otimes \phi(x(t))] dt.$$

Finally, we can take the transpose of both sides, apply our definitions of Y, Z , and use symmetry of Z to get

$$[Z + \lambda I]C^T = Y.$$

REFERENCES

- Romeo Alexander and Dimitrios Giannakis. Operator-theoretic framework for forecasting nonlinear time series with kernel analog techniques. *Physica D: Nonlinear Phenomena*, 409:132520, August 2020. ISSN 0167-2789. doi: 10.1016/j.physd.2020.132520. URL <http://www.sciencedirect.com/science/article/pii/S016727891930377X>.
- Ranjan Anantharaman, Yingbo Ma, Shashi Gowda, Chris Laughman, Viral Shah, Alan Edelman, and Chris Rackauckas. Accelerating Simulation of Stiff Nonlinear Systems using Continuous-Time Echo State Networks. October 2020. URL <https://arxiv.org/abs/2010.04004v6>.
- Eric Aislan Antonelo, Eduardo Camponogara, Laio Oriel Seman, Eduardo Rehbein de Souza, Jean P. Jordanou, and Jomi F. Hubner. Physics-Informed Neural Nets-based Control. April 2021. URL <https://arxiv.org/abs/2104.02556v1>.
- Mark Asch, Marc Bocquet, and Maëlle Nodet. *Data assimilation: methods, algorithms, and applications*. SIAM, 2016.
- Yunhao Ba, Guangyuan Zhao, and Achuta Kadambi. Blending Diverse Physical Priors with Neural Networks. *arXiv:1910.00201 [cs, stat]*, October 2019. URL <http://arxiv.org/abs/1910.00201>. arXiv: 1910.00201.
- Dzmitry Bahdanau, Kyunghyun Cho, and Yoshua Bengio. Neural Machine Translation by Jointly Learning to Align and Translate. *arXiv:1409.0473 [cs, stat]*, May 2016. URL <http://arxiv.org/abs/1409.0473>. arXiv: 1409.0473.
- Wael Bahsoun, Ian Melbourne, and Marks Ruziboev. Variance continuity for Lorenz flows. In *Annales Henri Poincaré*, volume 21, pages 1873–1892. Springer, 2020. Issue: 6.

- Randall D. Beer. On the Dynamics of Small Continuous-Time Recurrent Neural Networks. *Adaptive Behavior*, 3(4):469–509, March 1995. ISSN 1059-7123, 1741-2633. doi: 10.1177/105971239500300405. URL <http://journals.sagepub.com/doi/10.1177/105971239500300405>.
- Alain Bensoussan, Jacques-Louis Lions, and George Papanicolaou. *Asymptotic analysis for periodic structures*, volume 374. American Mathematical Soc., 2011.
- José Bento, Morteza Ibrahimi, and Andrea Montanari. Information theoretic limits on learning stochastic differential equations. In *2011 IEEE International Symposium on Information Theory Proceedings*, pages 855–859. IEEE, 2011.
- Tom Beucler, Michael Pritchard, Stephan Rasp, Jordan Ott, Pierre Baldi, and Pierre Gentine. Enforcing Analytic Constraints in Neural Networks Emulating Physical Systems. *Physical Review Letters*, 126(9):098302, 2021. Publisher: APS.
- Kaushik Bhattacharya, Bamdad Hosseini, Nikola B. Kovachki, and Andrew M. Stuart. Model Reduction and Neural Networks for Parametric PDEs. *arXiv:2005.03180 [cs, math, stat]*, May 2020. URL <http://arxiv.org/abs/2005.03180>. arXiv: 2005.03180.
- Marc Bocquet, Julien Brajard, Alberto Carrassi, and Laurent Bertino. Bayesian inference of chaotic dynamics by merging data assimilation, machine learning and expectation-maximization. *Foundations of Data Science*, 2(1):55, 2020. doi: 10.3934/fods.2020004. URL <https://www.aims sciences.org/article/doi/10.3934/fods.2020004>. Company: Foundations of Data Science Distributor: Foundations of Data Science Institution: Foundations of Data Science Label: Foundations of Data Science Publisher: American Institute of Mathematical Sciences.
- Francesco Borra, Angelo Vulpiani, and Massimo Cencini. Effective models and predictability of chaotic multiscale systems via machine learning. *Physical Review E*, 102(5):052203, November 2020. doi: 10.1103/PhysRevE.102.052203. URL <https://link.aps.org/doi/10.1103/PhysRevE.102.052203>. Publisher: American Physical Society.
- Julien Brajard, Alberto Carrassi, Marc Bocquet, and Laurent Bertino. Combining data assimilation and machine learning to emulate a dynamical model from sparse and noisy observations: a case study with the Lorenz 96 model. *Journal of Computational Science*, 44:101171, July 2020. ISSN 18777503. doi: 10.1016/j.jocs.2020.101171. URL <http://arxiv.org/abs/2001.01520>. arXiv: 2001.01520.
- Julien Brajard, Alberto Carrassi, Marc Bocquet, and Laurent Bertino. Combining data assimilation and machine learning to infer unresolved scale parametrization. *Philosophical Transactions of the Royal Society A: Mathematical, Physical and Engineering Sciences*, 379(2194):20200086, April 2021. doi: 10.1098/rsta.2020.0086. URL <https://royalsocietypublishing.org/doi/full/10.1098/rsta.2020.0086>. Publisher: Royal Society.
- N. D. Brenowitz and C. S. Bretherton. Prognostic Validation of a Neural Network Unified Physics Parameterization. *Geophysical Research Letters*, 45(12):6289–6298, 2018. ISSN 1944-8007. doi: <https://doi.org/10.1029/2018GL078510>. URL <https://agupubs.onlinelibrary.wiley.com/doi/abs/10.1029/2018GL078510>. eprint: <https://agupubs.onlinelibrary.wiley.com/doi/pdf/10.1029/2018GL078510>.
- Steven L. Brunton, Joshua L. Proctor, and J. Nathan Kutz. Discovering governing equations from data by sparse identification of nonlinear dynamical systems. *Proceedings of the National Academy of Sciences*, 113(15):3932–3937, April 2016.

- ISSN 0027-8424, 1091-6490. doi: 10.1073/pnas.1517384113. URL <https://www.pnas.org/content/113/15/3932>. Publisher: National Academy of Sciences Section: Physical Sciences.
- Dmitry Burov, Dimitrios Giannakis, Krithika Manohar, and Andrew Stuart. Kernel Analog Forecasting: Multiscale Test Problems. *arXiv:2005.06623 [physics, stat]*, May 2020. URL <http://arxiv.org/abs/2005.06623>. arXiv: 2005.06623.
- Kathleen Champion, Bethany Lusch, J. Nathan Kutz, and Steven L. Brunton. Data-driven discovery of coordinates and governing equations. *Proceedings of the National Academy of Sciences*, 116(45):22445–22451, November 2019. ISSN 0027-8424, 1091-6490. doi: 10.1073/pnas.1906995116. URL <https://www.pnas.org/content/116/45/22445>. Publisher: National Academy of Sciences Section: Physical Sciences.
- Bo Chang, Minmin Chen, Eldad Haber, and Ed H. Chi. AntisymmetricRNN: A Dynamical System View on Recurrent Neural Networks. *arXiv:1902.09689 [cs, stat]*, February 2019. URL <http://arxiv.org/abs/1902.09689>. arXiv: 1902.09689.
- Ashesh Chattopadhyay, Pedram Hassanzadeh, and Devika Subramanian. Data-driven predictions of a multiscale Lorenz 96 chaotic system using machine-learning methods: reservoir computing, artificial neural network, and long short-term memory network. *Nonlinear Processes in Geophysics*, 27(3):373–389, July 2020a. ISSN 1023-5809. doi: <https://doi.org/10.5194/npg-27-373-2020>. URL <https://npg.copernicus.org/articles/27/373/2020/>. Publisher: Copernicus GmbH.
- Ashesh Chattopadhyay, Adam Subel, and Pedram Hassanzadeh. Data-Driven Super-Parameterization Using Deep Learning: Experimentation With Multiscale Lorenz 96 Systems and Transfer Learning. *Journal of Advances in Modeling Earth Systems*, 12(11):e2020MS002084, 2020b. ISSN 1942-2466. doi: <https://doi.org/10.1029/2020MS002084>. URL <https://agupubs.onlinelibrary.wiley.com/doi/abs/10.1029/2020MS002084>. eprint: <https://agupubs.onlinelibrary.wiley.com/doi/pdf/10.1029/2020MS002084>.
- Yifan Chen, Bamdad Hosseini, Houman Owhadi, and Andrew M. Stuart. Solving and Learning Nonlinear PDEs with Gaussian Processes. *arXiv:2103.12959 [cs, math, stat]*, March 2021. URL <http://arxiv.org/abs/2103.12959>. arXiv: 2103.12959.
- Oksana A Chkrebtii, David A Campbell, Ben Calderhead, Mark A Girolami, and others. Bayesian solution uncertainty quantification for differential equations. *Bayesian Analysis*, 11(4):1239–1267, 2016. Publisher: International Society for Bayesian Analysis.
- Kyunghyun Cho, Bart van Merriënboer, Caglar Gulcehre, Dzmitry Bahdanau, Fethi Bougares, Holger Schwenk, and Yoshua Bengio. Learning Phrase Representations using RNN Encoder-Decoder for Statistical Machine Translation. *arXiv:1406.1078 [cs, stat]*, September 2014. URL <http://arxiv.org/abs/1406.1078>. arXiv: 1406.1078.
- Alexandre J Chorin, Ole H Hald, and Raz Kupferman. Optimal prediction and the Mori–Zwanzig representation of irreversible processes. *Proceedings of the National Academy of Sciences*, 97(7):2968–2973, 2000. Publisher: National Acad Sciences.
- David Colton and Rainer Kress. *Inverse Acoustic and Electromagnetic Scattering Theory*. Applied Mathematical Sciences. Springer-Verlag, New York, 3 edition, 2013. ISBN 978-1-4614-4941-6. doi: 10.1007/978-1-4614-4942-3. URL <https://>

- [//www.springer.com/gp/book/9781461449416](http://www.springer.com/gp/book/9781461449416).
- G. Cybenko. Approximation by superpositions of a sigmoidal function. *Mathematics of Control, Signals and Systems*, 2(4):303–314, December 1989. ISSN 1435-568X. doi: 10.1007/BF02551274. URL <https://doi.org/10.1007/BF02551274>.
- Eric Darve, Jose Solomon, and Amirali Kia. Computing generalized Langevin equations and generalized Fokker–Planck equations. *Proceedings of the National Academy of Sciences*, 106(27):10884–10889, 2009. Publisher: National Acad Sciences.
- Ronald A. DeVore and George G. Lorentz. *Constructive Approximation*. Grundlehren der mathematischen Wissenschaften. Springer-Verlag, Berlin Heidelberg, 1993. ISBN 978-3-540-50627-0. URL <https://www.springer.com/gp/book/9783540506270>.
- J. R. Dormand and P. J. Prince. A family of embedded Runge-Kutta formulae. *Journal of Computational and Applied Mathematics*, 6(1):19–26, March 1980. ISSN 0377-0427. doi: 10.1016/0771-050X(80)90013-3. URL <https://www.sciencedirect.com/science/article/pii/0771050X80900133>.
- Karthik Duraisamy, Gianluca Iaccarino, and Heng Xiao. Turbulence modeling in the age of data. *Annual Review of Fluid Mechanics*, 51:357–377, 2019. Publisher: Annual Reviews.
- Weinan E, Chao Ma, and Lei Wu. A Priori Estimates of the Population Risk for Two-layer Neural Networks. *Communications in Mathematical Sciences*, 17(5):1407–1425, 2019. ISSN 15396746, 19450796. doi: 10.4310/CMS.2019.v17.n5.a11. URL <http://arxiv.org/abs/1810.06397>. arXiv: 1810.06397.
- N. Benjamin Erichson, Omri Azencot, Alejandro Queiruga, Liam Hodgkinson, and Michael W. Mahoney. Lipschitz Recurrent Neural Networks. *arXiv:2006.12070 [cs, math, stat]*, October 2020. URL <http://arxiv.org/abs/2006.12070>. arXiv: 2006.12070.
- Alban Farchi, Patrick Laloyaux, Massimo Bonavita, and Marc Bocquet. Using machine learning to correct model error in data assimilation and forecast applications. *arXiv:2010.12605 [physics, stat]*, May 2021. URL <http://arxiv.org/abs/2010.12605>. arXiv: 2010.12605.
- Ibrahim Fatkullin and Eric Vanden-Eijnden. A computational strategy for multiscale systems with applications to Lorenz 96 model. *Journal of Computational Physics*, 200(2):605–638, 2004. Publisher: Elsevier.
- Brian A. Freno and Kevin T. Carlberg. Machine-learning error models for approximate solutions to parameterized systems of nonlinear equations. *Computer Methods in Applied Mechanics and Engineering*, 348:250–296, May 2019. ISSN 0045-7825. doi: 10.1016/j.cma.2019.01.024. URL <https://www.sciencedirect.com/science/article/pii/S0045782519300490>.
- Roger Frigola, Yutian Chen, and Carl Edward Rasmussen. Variational Gaussian Process State-Space Models. *Advances in Neural Information Processing Systems*, 27, 2014. URL <https://proceedings.neurips.cc/paper/2014/hash/139f0874f2ded2e41b0393c4ac5644f7-Abstract.html>.
- Ken-ichi Funahashi and Yuichi Nakamura. Approximation of dynamical systems by continuous time recurrent neural networks. *Neural Networks*, 6(6):801–806, January 1993. ISSN 0893-6080. doi: 10.1016/S0893-6080(05)80125-X. URL <http://www.sciencedirect.com/science/article/pii/S089360800580125X>.

- Faheem Gilani, Dimitrios Giannakis, and John Harlim. Kernel-based prediction of non-Markovian time series. *Physica D: Nonlinear Phenomena*, 418:132829, April 2021. ISSN 0167-2789. doi: 10.1016/j.physd.2020.132829. URL <https://www.sciencedirect.com/science/article/pii/S0167278920308307>.
- R. González-García, R. Rico-Martínez, and I.G. Kevrekidis. Identification of distributed parameter systems: A neural net based approach. *Computers & Chemical Engineering*, 22:S965–S968, March 1998. ISSN 00981354. doi: 10.1016/S0098-1354(98)00191-4. URL <https://linkinghub.elsevier.com/retrieve/pii/S0098135498001914>.
- Ian Goodfellow, Yoshua Bengio, and Aaron Courville. *Deep Learning*. MIT Press, 2016.
- Georg A. Gottwald and Sebastian Reich. Supervised learning from noisy observations: Combining machine-learning techniques with data assimilation. *Physica D: Nonlinear Phenomena*, 423:132911, September 2021. ISSN 0167-2789. doi: 10.1016/j.physd.2021.132911. URL <https://www.sciencedirect.com/science/article/pii/S0167278921000695>.
- Ayoub Gouasmi, Eric J. Parish, and Karthik Duraisamy. A priori estimation of memory effects in reduced-order models of nonlinear systems using the Mori–Zwanzig formalism. *Proceedings of the Royal Society A: Mathematical, Physical and Engineering Sciences*, 473(2205):20170385, September 2017. doi: 10.1098/rspa.2017.0385. URL <https://royalsocietypublishing.org/doi/10.1098/rspa.2017.0385>. Publisher: Royal Society.
- Wojciech W. Grabowski. Coupling Cloud Processes with the Large-Scale Dynamics Using the Cloud-Resolving Convection Parameterization (CRCP). *Journal of the Atmospheric Sciences*, 58(9):978–997, May 2001. ISSN 0022-4928, 1520-0469. doi: 10.1175/1520-0469(2001)058<0978:CCPWT1>2.0.CO;2. URL https://journals.ametsoc.org/view/journals/atmsc/58/9/1520-0469_2001_058_0978_ccpwt1_2.0.co_2.xml. Publisher: American Meteorological Society Section: Journal of the Atmospheric Sciences.
- Lyudmila Grigoryeva and Juan-Pablo Ortega. Echo state networks are universal. *arXiv:1806.00797 [cs]*, August 2018. URL <http://arxiv.org/abs/1806.00797>. arXiv: 1806.00797.
- Geoffrey Grimmett and David Stirzaker. *Probability and random processes*. Oxford university press, 2020.
- Abhinav Gupta and Pierre F. J. Lermusiaux. Neural Closure Models for Dynamical Systems. *arXiv:2012.13869 [physics]*, May 2021. URL <http://arxiv.org/abs/2012.13869>. arXiv: 2012.13869.
- Eldad Haber and Lars Ruthotto. Stable architectures for deep neural networks. *Inverse Problems*, 34(1):014004, December 2017. ISSN 0266-5611. doi: 10.1088/1361-6420/aa9a90. URL <https://doi.org/10.1088/1361-6420/aa9a90>. Publisher: IOP Publishing.
- Franz Hamilton, Alun L. Lloyd, and Kevin B. Flores. Hybrid modeling and prediction of dynamical systems. *PLOS Computational Biology*, 13(7):e1005655, July 2017. ISSN 1553-7358. doi: 10.1371/journal.pcbi.1005655. URL <https://journals.plos.org/ploscompbiol/article?id=10.1371/journal.pcbi.1005655>.
- Boumediene Hamzi and Houman Owadi. Learning dynamical systems from data: A simple cross-validation perspective, part I: Parametric kernel flows. *Physica D: Nonlinear Phenomena*, 421:132817, July 2021. ISSN 01672789. doi: 10.1016/j.

- physd.2020.132817. URL <https://linkinghub.elsevier.com/retrieve/pii/S0167278920308186>.
- John Harlim, Shixiao W. Jiang, Senwei Liang, and Haizhao Yang. Machine learning for prediction with missing dynamics. *Journal of Computational Physics*, 428: 109922, March 2021. ISSN 0021-9991. doi: 10.1016/j.jcp.2020.109922. URL <https://www.sciencedirect.com/science/article/pii/S0021999120306963>.
- Simon Haykin, Jose C. Principe, Terrence J. Sejnowski, and John McWhirter. Modeling Large Dynamical Systems with Dynamical Consistent Neural Networks. In *New Directions in Statistical Signal Processing: From Systems to Brains*, pages 203–241. MIT Press, 2007. ISBN 978-0-262-25631-5. URL <https://ieeexplore.ieee.org/document/6282085>. Conference Name: New Directions in Statistical Signal Processing: From Systems to Brains.
- Carmen Hijón, Pep Español, Eric Vanden-Eijnden, and Rafael Delgado-Buscalioni. Mori–Zwanzig formalism as a practical computational tool. *Faraday discussions*, 144:301–322, 2010. Publisher: Royal Society of Chemistry.
- Sepp Hochreiter and Jürgen Schmidhuber. Long Short-term Memory. *Neural computation*, 9:1735–80, December 1997. doi: 10.1162/neco.1997.9.8.1735.
- Mark Holland and Ian Melbourne. Central limit theorems and invariance principles for Lorenz attractors. *Journal of the London Mathematical Society*, 76(2):345–364, 2007. Publisher: Oxford University Press.
- Fabício P. Härter and Haroldo Fraga de Campos Velho. Data Assimilation Procedure by Recurrent Neural Network. *Engineering Applications of Computational Fluid Mechanics*, 6(2):224–233, January 2012. ISSN 1994-2060. doi: 10.1080/19942060.2012.11015417. URL <https://doi.org/10.1080/19942060.2012.11015417>. Publisher: Taylor & Francis eprint: <https://doi.org/10.1080/19942060.2012.11015417>.
- Herbert Jaeger. The” echo state” approach to analysing and training recurrent neural networks-with an erratum note’. *Bonn, Germany: German National Research Center for Information Technology GMD Technical Report*, 148, January 2001.
- Xiaowei Jia, Jared Willard, Anuj Karpatne, Jordan S. Read, Jacob A. Zwart, Michael Steinbach, and Vipin Kumar. Physics-Guided Machine Learning for Scientific Discovery: An Application in Simulating Lake Temperature Profiles. *ACM/IMS Transactions on Data Science*, 2(3):20:1–20:26, May 2021. ISSN 2691-1922. doi: 10.1145/3447814. URL <https://doi.org/10.1145/3447814>.
- Kadierdan Kaheman, Eurika Kaiser, Benjamin Strom, J. Nathan Kutz, and Steven L. Brunton. Learning Discrepancy Models From Experimental Data. *arXiv:1909.08574 [cs, eess, stat]*, September 2019. URL <http://arxiv.org/abs/1909.08574>. arXiv: 1909.08574.
- Kadierdan Kaheman, Steven L. Brunton, and J. Nathan Kutz. Automatic Differentiation to Simultaneously Identify Nonlinear Dynamics and Extract Noise Probability Distributions from Data. *arXiv:2009.08810 [cs, eess, math]*, September 2020. URL <http://arxiv.org/abs/2009.08810>. arXiv: 2009.08810.
- Jari Kaipio and E. Somersalo. *Statistical and Computational Inverse Problems*. Applied Mathematical Sciences. Springer-Verlag, New York, 2005. ISBN 978-0-387-22073-4. doi: 10.1007/b138659. URL <https://www.springer.com/gp/book/9780387220734>.

- J. Nagoor Kani and Ahmed H. Elsheikh. DR-RNN: A deep residual recurrent neural network for model reduction. *arXiv:1709.00939 [cs]*, September 2017. URL <http://arxiv.org/abs/1709.00939>. arXiv: 1709.00939.
- K. Kashinath, M. Mustafa, A. Albert, J-L. Wu, C. Jiang, S. Esmailzadeh, K. Azizadenesheli, R. Wang, A. Chattopadhyay, A. Singh, A. Manepalli, D. Chirila, R. Yu, R. Walters, B. White, H. Xiao, H. A. Tchelepi, P. Marcus, A. Anandkumar, P. Hassanzadeh, and null Prabhat. Physics-informed machine learning: case studies for weather and climate modelling. *Philosophical Transactions of the Royal Society A: Mathematical, Physical and Engineering Sciences*, 379(2194):20200093, April 2021. doi: 10.1098/rsta.2020.0093. URL <https://royalsocietypublishing.org/doi/full/10.1098/rsta.2020.0093>. Publisher: Royal Society.
- Marat F. Khairoutdinov and David A. Randall. A cloud resolving model as a cloud parameterization in the NCAR Community Climate System Model: Preliminary results. *Geophysical Research Letters*, 28(18):3617–3620, 2001. ISSN 1944-8007. doi: <https://doi.org/10.1029/2001GL013552>. URL <https://agupubs.onlinelibrary.wiley.com/doi/abs/10.1029/2001GL013552>. eprint: <https://agupubs.onlinelibrary.wiley.com/doi/pdf/10.1029/2001GL013552>.
- Juš Kocijan. *Modelling and Control of Dynamic Systems Using Gaussian Process Models*. Advances in Industrial Control. Springer International Publishing, 2016. ISBN 978-3-319-21020-9. doi: 10.1007/978-3-319-21021-6. URL <https://www.springer.com/gp/book/9783319210209>.
- Milan Korda, Mihai Putinar, and Igor Mezić. Data-driven spectral analysis of the Koopman operator. *Applied and Computational Harmonic Analysis*, 48(2): 599–629, 2020. Publisher: Elsevier.
- K. Krischer, R. Rico-Martínez, I. G. Kevrekidis, H. H. Rotermund, G. Ertl, and J. L. Hudson. Model identification of a spatiotemporally varying catalytic reaction. *AIChE Journal*, 39(1):89–98, January 1993. ISSN 0001-1541, 1547-5905. doi: 10.1002/aic.690390110. URL <http://doi.wiley.com/10.1002/aic.690390110>.
- S. Kullback and R. A. Leibler. On Information and Sufficiency. *The Annals of Mathematical Statistics*, 22(1):79–86, March 1951. ISSN 0003-4851, 2168-8990. doi: 10.1214/aoms/1177729694. URL <https://projecteuclid.org/journals/annals-of-mathematical-statistics/volume-22/issue-1/On-Information-and-Sufficiency/10.1214/aoms/1177729694.full>. Publisher: Institute of Mathematical Statistics.
- Yury A. Kutoyants. *Statistical Inference for Ergodic Diffusion Processes*. Springer Series in Statistics. Springer-Verlag, London, 2004. ISBN 978-1-85233-759-9. doi: 10.1007/978-1-4471-3866-2. URL <https://www.springer.com/gp/book/9781852337599>.
- I. E. Lagaris, A. Likas, and D. I. Fotiadis. Artificial Neural Networks for Solving Ordinary and Partial Differential Equations. *IEEE Transactions on Neural Networks*, 9(5):987–1000, September 1998. ISSN 10459227. doi: 10.1109/72.712178. URL <http://arxiv.org/abs/physics/9705023>. arXiv: physics/9705023.
- Kody Law, Andrew Stuart, and Kostas Zygalakis. Data assimilation. *Cham, Switzerland: Springer*, 214, 2015. Publisher: Springer.
- Youning Lei, Jian Hu, and Jianpeng Ding. A hybrid model based on deep LSTM for predicting high-dimensional chaotic systems. *arXiv:2002.00799 [cs, eess]*, January 2020. URL <http://arxiv.org/abs/2002.00799>. arXiv: 2002.00799.

- Zhen Li, Hee Sun Lee, Eric Darve, and George Em Karniadakis. Computing the non-Markovian coarse-grained interactions derived from the Mori–Zwanzig formalism in molecular systems: Application to polymer melts. *The Journal of Chemical Physics*, 146(1):014104, 2017. Publisher: AIP Publishing LLC.
- Zhong Li, Jiequn Han, Weinan E, and Qianxiao Li. On the Curse of Memory in Recurrent Neural Networks: Approximation and Optimization Analysis. *arXiv:2009.07799 [cs, math, stat]*, September 2020. URL <http://arxiv.org/abs/2009.07799>. arXiv: 2009.07799.
- Zongyi Li, Nikola Kovachki, Kamyar Azizzadenesheli, Burigede Liu, Kaushik Bhattacharya, Andrew Stuart, and Anima Anandkumar. Fourier Neural Operator for Parametric Partial Differential Equations. *arXiv:2010.08895 [cs, math]*, March 2021. URL <http://arxiv.org/abs/2010.08895>. arXiv: 2010.08895.
- Kevin K. Lin and Fei Lu. Data-driven model reduction, Wiener projections, and the Koopman–Mori–Zwanzig formalism. *Journal of Computational Physics*, 424:109864, January 2021. ISSN 0021-9991. doi: 10.1016/j.jcp.2020.109864. URL <https://www.sciencedirect.com/science/article/pii/S0021999120306380>.
- Ori Linial, Neta Ravid, Danny Eytan, and Uri Shalit. Generative ODE modeling with known unknowns. In *Proceedings of the Conference on Health, Inference, and Learning*, CHIL ’21, pages 79–94, New York, NY, USA, April 2021. Association for Computing Machinery. ISBN 978-1-4503-8359-2. doi: 10.1145/3450439.3451866. URL <https://doi.org/10.1145/3450439.3451866>.
- E. Lorenz. Predictability—A problem partly solved. *Proc. Seminar on Predictability, Reading, UK, ECMWF, 1996*, 1996. URL <https://ci.nii.ac.jp/naid/10015392260/en/>.
- Edward N. Lorenz. Deterministic Nonperiodic Flow. *Journal of the Atmospheric Sciences*, 20(2):130–141, March 1963. ISSN 0022-4928, 1520-0469. doi: 10.1175/1520-0469(1963)020<0130:DNF>2.0.CO;2. URL https://journals.ametsoc.org/view/journals/atmsc/20/2/1520-0469_1963_020_0130_dnf_2_0_co_2.xml. Publisher: American Meteorological Society Section: Journal of the Atmospheric Sciences.
- Robert J. Lovelett, José L. Avalos, and Ioannis G. Kevrekidis. Partial Observations and Conservation Laws: Gray-Box Modeling in Biotechnology and Optogenetics. *Industrial & Engineering Chemistry Research*, 59(6):2611–2620, February 2020. ISSN 0888-5885. doi: 10.1021/acs.iecr.9b04507. URL <https://doi.org/10.1021/acs.iecr.9b04507>. Publisher: American Chemical Society.
- Lu Lu, Pengzhan Jin, and George Em Karniadakis. DeepONet: Learning nonlinear operators for identifying differential equations based on the universal approximation theorem of operators. *arXiv:1910.03193 [cs, stat]*, April 2020. URL <http://arxiv.org/abs/1910.03193>. arXiv: 1910.03193.
- Zhixin Lu, Brian R. Hunt, and Edward Ott. Attractor reconstruction by machine learning. *Chaos: An Interdisciplinary Journal of Nonlinear Science*, 28(6):061104, June 2018. ISSN 1054-1500. doi: 10.1063/1.5039508. URL <https://aip.scitation.org/doi/10.1063/1.5039508>. Publisher: American Institute of Physics.
- Mantas Lukoševičius and Herbert Jaeger. Reservoir computing approaches to recurrent neural network training. *Computer Science Review*, 3(3):127–149, August 2009. ISSN 1574-0137. doi: 10.1016/j.cosrev.2009.03.005. URL <https://www.sciencedirect.com/science/article/pii/S1574013709000173>.

- Chao Ma, Jianchun Wang, and Weinan E. Model Reduction with Memory and the Machine Learning of Dynamical Systems. *Communications in Computational Physics*, 25(4), 2019. ISSN 18152406. doi: 10.4208/cicp.OA-2018-0269. URL http://www.global-sci.com/intro/article_detail/cicp/12885.html.
- Romit Maulik, Bethany Lusch, and Prasanna Balaprakash. Reduced-order modeling of advection-dominated systems with recurrent neural networks and convolutional autoencoders. *Physics of Fluids*, 33(3):037106, March 2021. ISSN 1070-6631. doi: 10.1063/5.0039986. URL <https://aip.scitation.org/doi/abs/10.1063/5.0039986>. Publisher: American Institute of Physics.
- Kevin McGoff, Sayan Mukherjee, Andrew Nobel, and Natesh Pillai. Consistency of maximum likelihood estimation for some dynamical systems. *The Annals of Statistics*, 43(1):1–29, February 2015. ISSN 0090-5364, 2168-8966. doi: 10.1214/14-AOS1259. URL <https://projecteuclid.org/journals/annals-of-statistics/volume-43/issue-1/Consistency-of-maximum-likelihood-estimation-for-some-dynamical-systems/10.1214/14-AOS1259.full>. Publisher: Institute of Mathematical Statistics.
- Andrew C. Miller, Nicholas J. Foti, and Emily Fox. Learning Insulin-Glucose Dynamics in the Wild. *arXiv:2008.02852 [cs, stat]*, August 2020. URL <http://arxiv.org/abs/2008.02852>. arXiv: 2008.02852.
- Andrew C. Miller, Nicholas J. Foti, and Emily B. Fox. Breiman’s two cultures: You don’t have to choose sides. *arXiv:2104.12219 [cs, stat]*, April 2021. URL <http://arxiv.org/abs/2104.12219>. arXiv: 2104.12219.
- Jonas Mockus. *Bayesian Approach to Global Optimization: Theory and Applications*. Mathematics and its Applications. Springer Netherlands, 1989. ISBN 978-94-010-6898-7. doi: 10.1007/978-94-009-0909-0. URL <https://www.springer.com/gp/book/9789401068987>.
- Kumpati S. Narendra and Kannan Parthasarathy. Neural networks and dynamical systems. *International Journal of Approximate Reasoning*, 6(2):109–131, February 1992. ISSN 0888-613X. doi: 10.1016/0888-613X(92)90014-Q. URL <https://www.sciencedirect.com/science/article/pii/0888613X9290014Q>.
- Nicholas H. Nelsen and Andrew M. Stuart. The Random Feature Model for Input-Output Maps between Banach Spaces. *arXiv:2005.10224 [physics, stat]*, May 2020. URL <http://arxiv.org/abs/2005.10224>. arXiv: 2005.10224.
- Duong Nguyen, Said Ouala, Lucas Drumetz, and Ronan Fablet. EM-like Learning Chaotic Dynamics from Noisy and Partial Observations. *arXiv:1903.10335 [cs, stat]*, March 2019. URL <http://arxiv.org/abs/1903.10335>. arXiv: 1903.10335.
- Murphy Yuezhen Niu, Lior Horeish, and Isaac Chuang. Recurrent Neural Networks in the Eye of Differential Equations. *arXiv:1904.12933 [quant-ph, stat]*, April 2019. URL <http://arxiv.org/abs/1904.12933>. arXiv: 1904.12933.
- Paul A. O’Gorman and John G. Dwyer. Using Machine Learning to Parameterize Moist Convection: Potential for Modeling of Climate, Climate Change, and Extreme Events. *Journal of Advances in Modeling Earth Systems*, 10(10):2548–2563, 2018. ISSN 1942-2466. doi: <https://doi.org/10.1029/2018MS001351>. URL <https://agupubs.onlinelibrary.wiley.com/doi/abs/10.1029/2018MS001351>. eprint: <https://agupubs.onlinelibrary.wiley.com/doi/pdf/10.1029/2018MS001351>.
- Eric J Parish and Karthik Duraisamy. A dynamic subgrid scale model for large eddy simulations based on the Mori–Zwanzig formalism. *Journal of Computational*

- Physics*, 349:154–175, 2017. Publisher: Elsevier.
- Jaideep Pathak, Brian Hunt, Michelle Girvan, Zhixin Lu, and Edward Ott. Model-Free Prediction of Large Spatiotemporally Chaotic Systems from Data: A Reservoir Computing Approach. *Physical Review Letters*, 120(2):024102, January 2018a. ISSN 0031-9007, 1079-7114. doi: 10.1103/PhysRevLett.120.024102. URL <https://link.aps.org/doi/10.1103/PhysRevLett.120.024102>.
- Jaideep Pathak, Alexander Wikner, Rebeckah Fussell, Sarthak Chandra, Brian R. Hunt, Michelle Girvan, and Edward Ott. Hybrid forecasting of chaotic processes: Using machine learning in conjunction with a knowledge-based model. *Chaos: An Interdisciplinary Journal of Nonlinear Science*, 28(4):041101, April 2018b. ISSN 1054-1500. doi: 10.1063/1.5028373. URL <https://aip.scitation.org/doi/10.1063/1.5028373>.
- Grigoris Pavliotis and Andrew Stuart. *Multiscale methods: averaging and homogenization*. Springer Science & Business Media, 2008.
- Matthew Plumlee. Bayesian Calibration of Inexact Computer Models. *Journal of the American Statistical Association*, 112(519):1274–1285, July 2017. ISSN 0162-1459, 1537-274X. doi: 10.1080/01621459.2016.1211016. URL <https://www.tandfonline.com/doi/full/10.1080/01621459.2016.1211016>.
- Matthew Plumlee and V. Roshan Joseph. Orthogonal Gaussian process models. *Statistica Sinica*, 2017. ISSN 10170405. doi: 10.5705/ss.202015.0404. URL <http://www3.stat.sinica.edu.tw/statistica/J28N2/J28N23/J28N23.html>.
- Manuel Pulido, Pierre Tandeo, Marc Bocquet, Alberto Carrassi, and Magdalena Lucini. Stochastic parameterization identification using ensemble Kalman filtering combined with maximum likelihood methods. *Tellus A: Dynamic Meteorology and Oceanography*, 70(1):1–17, 2018. Publisher: Taylor & Francis.
- Zhaozhi Qian, William R. Zame, Lucas M. Fleuren, Paul Elbers, and Mihaela van der Schaar. Integrating Expert ODEs into Neural ODEs: Pharmacology and Disease Progression. *arXiv:2106.02875 [cs, stat]*, June 2021. URL <http://arxiv.org/abs/2106.02875>. arXiv: 2106.02875.
- Alejandro F. Queiruga, N. Benjamin Erichson, Dane Taylor, and Michael W. Mahoney. Continuous-in-Depth Neural Networks. *arXiv:2008.02389 [cs, math, stat]*, August 2020. URL <http://arxiv.org/abs/2008.02389>. arXiv: 2008.02389.
- Christopher Rackauckas, Yingbo Ma, Julius Martensen, Collin Warner, Kirill Zubov, Rohit Supekar, Dominic Skinner, Ali Ramadhan, and Alan Edelman. Universal Differential Equations for Scientific Machine Learning. *arXiv:2001.04385 [cs, math, q-bio, stat]*, August 2020. URL <http://arxiv.org/abs/2001.04385>. arXiv: 2001.04385.
- Christopher Rackauckas, Roshan Sharma, and Bernt Lie. Hybrid Mechanistic + Neural Model of Laboratory Helicopter. pages 264–271, March 2021. doi: 10.3384/ecp20176264. URL https://ep.liu.se/en/conference-article.aspx?series=ecp&issue=176&Article_No=37.
- Ali Rahimi and Benjamin Recht. Random Features for Large-Scale Kernel Machines. In J. Platt, D. Koller, Y. Singer, and S. Roweis, editors, *Advances in Neural Information Processing Systems*, volume 20. Curran Associates, Inc., 2008a. URL <https://proceedings.neurips.cc/paper/2007/file/013a006f03dbc5392effeb8f18fda755-Paper.pdf>.
- Ali Rahimi and Benjamin Recht. Uniform approximation of functions with random bases. In *2008 46th Annual Allerton Conference on Communication, Control,*

- and Computing*, pages 555–561. IEEE, 2008b.
- Ali Rahimi and Benjamin Recht. Weighted sums of random kitchen sinks: replacing minimization with randomization in learning. In *Nips*, pages 1313–1320. Citeseer, 2008c.
- M. Raissi, P. Perdikaris, and G. E. Karniadakis. Physics-informed neural networks: A deep learning framework for solving forward and inverse problems involving nonlinear partial differential equations. *Journal of Computational Physics*, 378:686–707, February 2019. ISSN 0021-9991. doi: 10.1016/j.jcp.2018.10.045. URL <https://www.sciencedirect.com/science/article/pii/S0021999118307125>.
- Maziar Raissi, Paris Perdikaris, and George Em Karniadakis. Multistep Neural Networks for Data-driven Discovery of Nonlinear Dynamical Systems. *arXiv:1801.01236 [nlin, physics:physics, stat]*, January 2018. URL <http://arxiv.org/abs/1801.01236>. arXiv: 1801.01236.
- Carl Edward Rasmussen and Christopher K. I. Williams. *Gaussian processes for machine learning*. Adaptive computation and machine learning. MIT Press, Cambridge, Mass, 2006. ISBN 978-0-262-18253-9. OCLC: ocm61285753.
- Stephan Rasp, Michael S. Pritchard, and Pierre Gentine. Deep learning to represent subgrid processes in climate models. *Proceedings of the National Academy of Sciences*, 115(39):9684–9689, September 2018. ISSN 0027-8424, 1091-6490. doi: 10.1073/pnas.1810286115. URL <https://www.pnas.org/content/115/39/9684>. ISBN: 9781810286112 Publisher: National Academy of Sciences Section: Physical Sciences.
- Sebastian Reich and Colin Cotter. *Probabilistic forecasting and Bayesian data assimilation*. Cambridge University Press, 2015.
- R. Rico-Martínez, I. G. Kevrekidis, M. C. Kube, and J. L. Hudson. Discrete- vs. Continuous-Time Nonlinear Signal Processing: Attractors, Transitions and Parallel Implementation Issues. In *1993 American Control Conference*, pages 1475–1479, San Francisco, CA, USA, June 1993. IEEE. ISBN 978-0-7803-0860-2. doi: 10.23919/ACC.1993.4793116. URL <https://ieeexplore.ieee.org/document/4793116/>.
- R. Rico-Martínez, J.S. Anderson, and I.G. Kevrekidis. Continuous-time nonlinear signal processing: a neural network based approach for gray box identification. In *Proceedings of IEEE Workshop on Neural Networks for Signal Processing*, pages 596–605, Ermioni, Greece, 1994. IEEE. ISBN 978-0-7803-2026-0. doi: 10.1109/NNSP.1994.366006. URL <http://ieeexplore.ieee.org/document/366006/>.
- R. Rico-Martínez, K. Krischer, I.G. Kevrekidis, M.C. Kube, and J.L. Hudson. DISCRETE- vs. CONTINUOUS-TIME NONLINEAR SIGNAL PROCESSING OF Cu ELECTRODISSOLUTION DATA. *Chemical Engineering Communications*, 118(1):25–48, November 1992. ISSN 0098-6445, 1563-5201. doi: 10.1080/00986449208936084. URL <https://www.tandfonline.com/doi/full/10.1080/00986449208936084>.
- Yulia Rubanova, Ricky T. Q. Chen, and David Duvenaud. Latent ODEs for Irregularly-Sampled Time Series. *arXiv:1907.03907 [cs, stat]*, July 2019. URL <http://arxiv.org/abs/1907.03907>. arXiv: 1907.03907.
- David E Rumelhart, Geoffrey E Hinton, and Ronald J Williams. Learning representations by back-propagating errors. *nature*, 323(6088):533–536, 1986. Publisher: Nature Publishing Group.

- Matteo Saveriano, Yuchao Yin, Pietro Falco, and Dongheui Lee. Data-efficient control policy search using residual dynamics learning. In *2017 IEEE/RSJ International Conference on Intelligent Robots and Systems (IROS)*, pages 4709–4715, September 2017. doi: 10.1109/IROS.2017.8206343. ISSN: 2153-0866.
- Hayden Schaeffer, Giang Tran, and Rachel Ward. Learning dynamical systems and bifurcation via group sparsity. *arXiv preprint arXiv:1709.01558*, 2017.
- Hayden Schaeffer, Giang Tran, and Rachel Ward. Extracting sparse high-dimensional dynamics from limited data. *SIAM Journal on Applied Mathematics*, 78(6):3279–3295, 2018. Publisher: SIAM.
- Hayden Schaeffer, Giang Tran, Rachel Ward, and Linan Zhang. Extracting structured dynamical systems using sparse optimization with very few samples. *Multiscale Modeling & Simulation*, 18(4):1435–1461, 2020. Publisher: SIAM.
- Tapio Schneider, Andrew M. Stuart, and Jin-Long Wu. Learning Stochastic Closures Using Ensemble Kalman Inversion. *arXiv:2004.08376 [physics, stat]*, April 2020. URL <http://arxiv.org/abs/2004.08376>. arXiv: 2004.08376.
- Anton Maximilian Schäfer and Hans-Georg Zimmermann. Recurrent Neural Networks are universal approximators. *International Journal of Neural Systems*, 17(4):253–263, August 2007. ISSN 0129-0657. doi: 10.1142/S0129065707001111.
- Skipper Seabold and Josef Perktold. statsmodels: Econometric and statistical modeling with python. In *9th Python in Science Conference*, 2010.
- Alex Sherstinsky. Fundamentals of Recurrent Neural Network (RNN) and Long Short-Term Memory (LSTM) network. *Physica D: Nonlinear Phenomena*, 404:132306, March 2020. ISSN 0167-2789. doi: 10.1016/j.physd.2019.132306. URL <http://www.sciencedirect.com/science/article/pii/S0167278919305974>.
- Guanya Shi, Xichen Shi, Michael O’Connell, Rose Yu, Kamyar Azizzadenesheli, Animashree Anandkumar, Yisong Yue, and Soon-Jo Chung. Neural Lander: Stable Drone Landing Control using Learned Dynamics. *arXiv:1811.08027 [cs]*, November 2018. URL <http://arxiv.org/abs/1811.08027>. arXiv: 1811.08027.
- Jonathan D. Smith, Kamyar Azizzadenesheli, and Zachary E. Ross. EikoNet: Solving the Eikonal Equation With Deep Neural Networks. *IEEE Transactions on Geoscience and Remote Sensing*, pages 1–12, 2020. ISSN 1558-0644. doi: 10.1109/TGRS.2020.3039165. Conference Name: IEEE Transactions on Geoscience and Remote Sensing.
- Peter D. Sottile, David Albers, Peter E. DeWitt, Seth Russell, J. N. Stroh, David P. Kao, Bonnie Adrian, Matthew E. Levine, Ryan Mooney, Lenny Larchick, Jean S. Kutner, Matthew K. Wynia, Jeffrey J. Glasheen, and Tellen D. Bennett. Real-Time Electronic Health Record Mortality Prediction During the COVID-19 Pandemic: A Prospective Cohort Study. *medRxiv*, page 2021.01.14.21249793, January 2021. doi: 10.1101/2021.01.14.21249793. URL <https://www.medrxiv.org/content/10.1101/2021.01.14.21249793v1>. Publisher: Cold Spring Harbor Laboratory Press.
- Langxuan Su and Sayan Mukherjee. A Large Deviation Approach to Posterior Consistency in Dynamical Systems. *arXiv:2106.06894 [math, stat]*, June 2021. URL <http://arxiv.org/abs/2106.06894>. arXiv: 2106.06894.
- Floris Takens. Detecting strange attractors in turbulence. In David Rand and Lai-Sang Young, editors, *Dynamical Systems and Turbulence, Warwick 1980*, Lecture Notes in Mathematics, pages 366–381, Berlin, Heidelberg, 1981. Springer. ISBN 978-3-540-38945-3. doi: 10.1007/BFb0091924.

- Zhihong Tan, Colleen M Kaul, Kyle G Pressel, Yair Cohen, Tapio Schneider, and João Teixeira. An extended eddy-diffusivity mass-flux scheme for unified representation of subgrid-scale turbulence and convection. *Journal of Advances in Modeling Earth Systems*, 10(3):770–800, 2018. Publisher: Wiley Online Library.
- Ramakrishna Tipireddy, Paris Perdikaris, Panos Stinis, and Alexandre Tartakovsky. A comparative study of physics-informed neural network models for learning unknown dynamics and constitutive relations. *arXiv:1904.04058 [physics]*, April 2019. URL <http://arxiv.org/abs/1904.04058>. arXiv: 1904.04058.
- Giang Tran and Rachel Ward. Exact recovery of chaotic systems from highly corrupted data. *Multiscale Modeling & Simulation*, 15(3):1108–1129, 2017. Publisher: SIAM.
- Jonathan H. Tu, Clarence W. Rowley, Dirk M. Luchtenburg, Steven L. Brunton, and J. Nathan Kutz. On dynamic mode decomposition: Theory and applications. *Journal of Computational Dynamics*, 1(2):391, 2014. doi: 10.3934/jcd.2014.1.391. URL <https://www.aims sciences.org/article/doi/10.3934/jcd.2014.1.391>. Company: Journal of Computational Dynamics Distributor: Journal of Computational Dynamics Institution: Journal of Computational Dynamics Label: Journal of Computational Dynamics Publisher: American Institute of Mathematical Sciences.
- Eric Vanden-Eijnden and others. Fast communications: Numerical techniques for multi-scale dynamical systems with stochastic effects. *Communications in Mathematical Sciences*, 1(2):385–391, 2003. Publisher: International Press of Boston.
- Vladimir Vapnik. *The nature of statistical learning theory*. Springer science & business media, 2013.
- Pauli Virtanen, Ralf Gommers, Travis E. Oliphant, Matt Haberland, Tyler Reddy, David Cournapeau, Evgeni Burovski, Pearu Peterson, Warren Weckesser, Jonathan Bright, Stéfan J. van der Walt, Matthew Brett, Joshua Wilson, K. Jarrod Millman, Nikolay Mayorov, Andrew R. J. Nelson, Eric Jones, Robert Kern, Eric Larson, C. J. Carey, Ilhan Polat, Yu Feng, Eric W. Moore, Jake VanderPlas, Denis Laxalde, Josef Perktold, Robert Cimrman, Ian Henriksen, E. A. Quintero, Charles R. Harris, Anne M. Archibald, Antônio H. Ribeiro, Fabian Pedregosa, and Paul van Mulbregt. SciPy 1.0: fundamental algorithms for scientific computing in Python. *Nature Methods*, 17(3):261–272, March 2020. ISSN 1548-7105. doi: 10.1038/s41592-019-0686-2. URL <https://www.nature.com/articles/s41592-019-0686-2>. Number: 3 Publisher: Nature Publishing Group.
- P.R. Vlachas, J. Pathak, B.R. Hunt, T.P. Sapsis, M. Girvan, E. Ott, and P. Koumoutsakos. Backpropagation algorithms and Reservoir Computing in Recurrent Neural Networks for the forecasting of complex spatiotemporal dynamics. *Neural Networks*, 126:191–217, June 2020. ISSN 08936080. doi: 10.1016/j.neunet.2020.02.016. URL <https://linkinghub.elsevier.com/retrieve/pii/S0893608020300708>.
- Jack Wang, Aaron Hertzmann, and David J. Fleet. Gaussian Process Dynamical Models. *Advances in Neural Information Processing Systems*, 18, 2005. URL <https://papers.nips.cc/paper/2005/hash/ccd45007df44dd0f12098f486e7e8a0f-Abstract.html>.

- Qian Wang, Nicolò Ripamonti, and Jan S Hesthaven. Recurrent neural network closure of parametric POD-Galerkin reduced-order models based on the Mori-Zwanzig formalism. *Journal of Computational Physics*, 410:109402, 2020. Publisher: Elsevier.
- Peter A. G. Watson. Applying machine learning to improve simulations of a chaotic dynamical system using empirical error correction. *arXiv:1904.10904 [nlin, physics:physics, stat]*, April 2019. URL <http://arxiv.org/abs/1904.10904>. arXiv: 1904.10904.
- Alexander Wikner, Jaideep Pathak, Brian Hunt, Michelle Girvan, Troy Arcomano, Istvan Szunyogh, Andrew Pomerance, and Edward Ott. Combining machine learning with knowledge-based modeling for scalable forecasting and subgrid-scale closure of large, complex, spatiotemporal systems. *Chaos: An Interdisciplinary Journal of Nonlinear Science*, 30(5):053111, May 2020. ISSN 1054-1500. doi: 10.1063/5.0005541. URL <https://aip.scitation.org/doi/10.1063/5.0005541>. Publisher: American Institute of Physics.
- J.A. Wilson and L.F.M. Zorzetto. A generalised approach to process state estimation using hybrid artificial neural network/mechanistic models. *Computers & Chemical Engineering*, 21(9):951–963, June 1997. ISSN 00981354. doi: 10.1016/S0098-1354(96)00336-5. URL <http://linkinghub.elsevier.com/retrieve/pii/S0098135496003365>.
- Armand Wirgin. The inverse crime. *arXiv:math-ph/0401050*, January 2004. URL <http://arxiv.org/abs/math-ph/0401050>. arXiv: math-ph/0401050.
- David H. Wolpert. Stacked generalization. *Neural Networks*, 5(2):241–259, January 1992. ISSN 0893-6080. doi: 10.1016/S0893-6080(05)80023-1. URL <https://www.sciencedirect.com/science/article/pii/S0893608005800231>.
- Alireza Yazdani, Lu Lu, Maziar Raissi, and George Em Karniadakis. Systems biology informed deep learning for inferring parameters and hidden dynamics. *PLOS Computational Biology*, 16(11):e1007575, November 2020. ISSN 1553-7358. doi: 10.1371/journal.pcbi.1007575. URL <https://journals.plos.org/ploscompbiol/article?id=10.1371/journal.pcbi.1007575>. Publisher: Public Library of Science.
- Zhong Yi Wan, Petr Karnakov, Petros Koumoutsakos, and Themistoklis P. Sapsis. Bubbles in turbulent flows: Data-driven, kinematic models with history terms. *International Journal of Multiphase Flow*, 129:103286, August 2020. ISSN 0301-9322. doi: 10.1016/j.ijmultiphaseflow.2020.103286. URL <http://www.sciencedirect.com/science/article/pii/S030193221930758X>.
- He Zhang, John Harlim, and Xiantao Li. Error Bounds of the Invariant Statistics in Machine Learning of Ergodic Itô Diffusions. *arXiv:2105.10102 [cs, math]*, May 2021. URL <http://arxiv.org/abs/2105.10102>. arXiv: 2105.10102.
- Jian Zhu and Masafumi Kamachi. An adaptive variational method for data assimilation with imperfect models. *Tellus A: Dynamic Meteorology and Oceanography*, 52(3):265–279, January 2000. ISSN null. doi: 10.3402/tellusa.v52i3.12265. URL <https://doi.org/10.3402/tellusa.v52i3.12265>. Publisher: Taylor & Francis. eprint: <https://doi.org/10.3402/tellusa.v52i3.12265>.
- Yuanran Zhu, Jason M Dominy, and Daniele Venturi. On the estimation of the Mori-Zwanzig memory integral. *Journal of Mathematical Physics*, 59(10):103501, 2018. Publisher: AIP Publishing LLC.

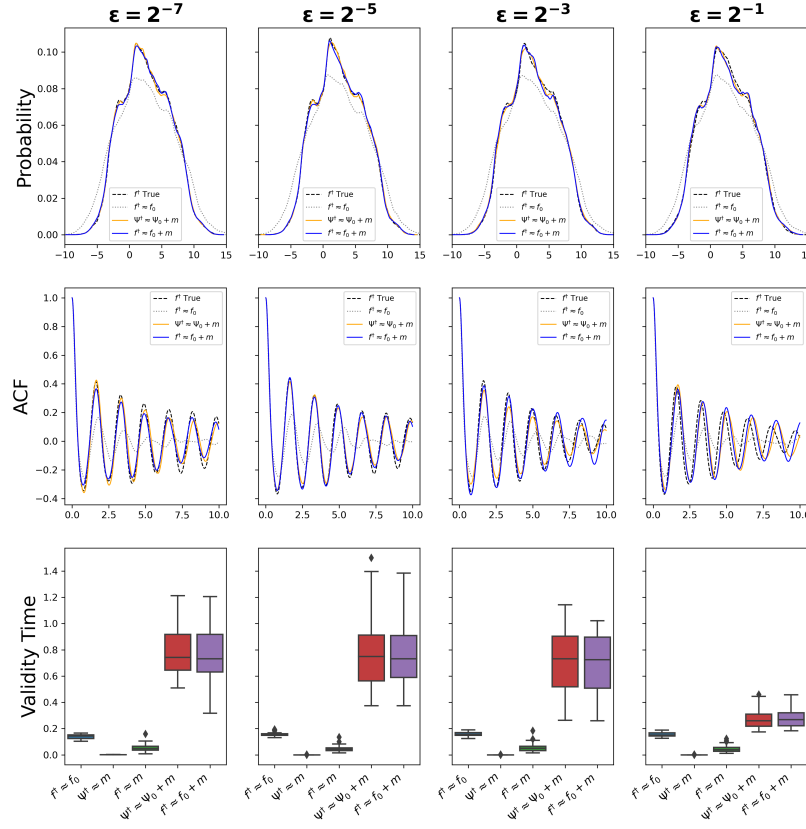


FIGURE 6. This figure shows the performance of different approaches to modeling the slow subsystem L96MS. In $f^\dagger \approx f_0$, we only use the nominal physics f_0 . In $\Psi^\dagger \approx m$ and $f^\dagger \approx m$, we try to learn the entire right-hand-side using only data (in discrete- and continuous-time settings, respectively). In $\Psi^\dagger \approx \Psi_0 + m$ and $f^\dagger \approx f_0 + m$, we focus on learning Markovian residuals for the known physics (in discrete- and continuous-time settings, respectively). We see that the data-only methods are inferior to using f_0 alone—this poor performance stresses the complexity and dimensionality of the system, as well as the impact of limited training data availability. However, the residual-based corrector methods substantially outperform the nominal physics according to all presented metrics: they better improve estimates of the invariant measure, the autocorrelation function, and trajectory forecasts. However, we see some decline in performance improvements from the Markovian approach for small scale-separation ($\varepsilon = 2^{-1}$). This deterioration is expected, as the Markovian assumption breaks down for larger values of ε .

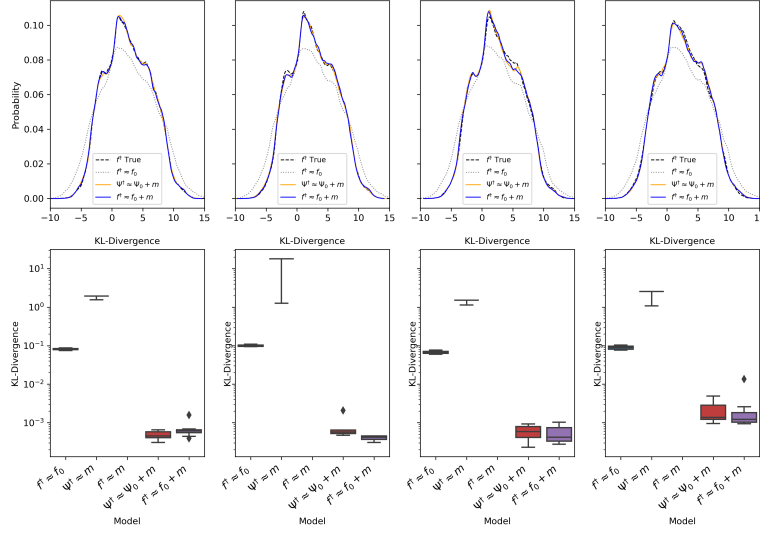


FIGURE 7. We quantify accuracy of our estimate of the invariant measure by computing the Kullback-Leibler divergence between the true and estimated densities. The boxplots show the distributions of KL-divergences, which come from different models, each trained on a different trajectory, and generated using an independent random feature set.

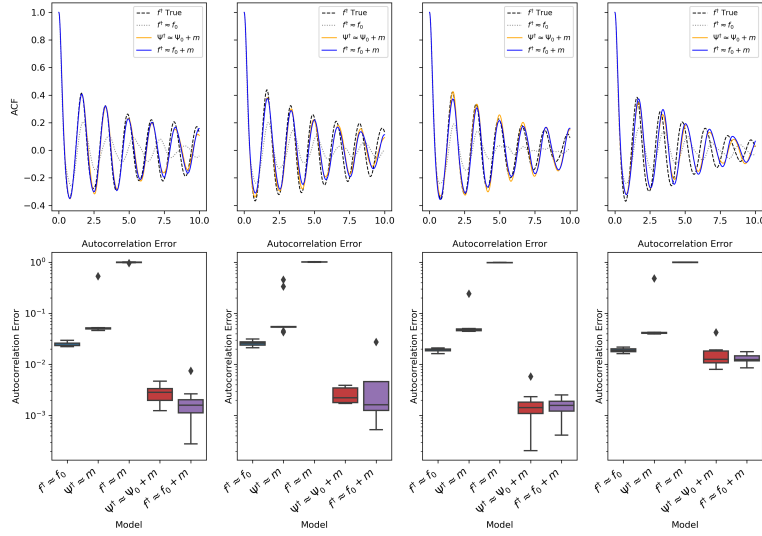


FIGURE 8. We quantify accuracy of our estimate of the autocorrelation function by computing the squared error between the true and approximate ACFs. The boxplots show the distributions of mean-squared-errors, which come from different models, each trained on a different trajectory, and generated using an independent random feature set.

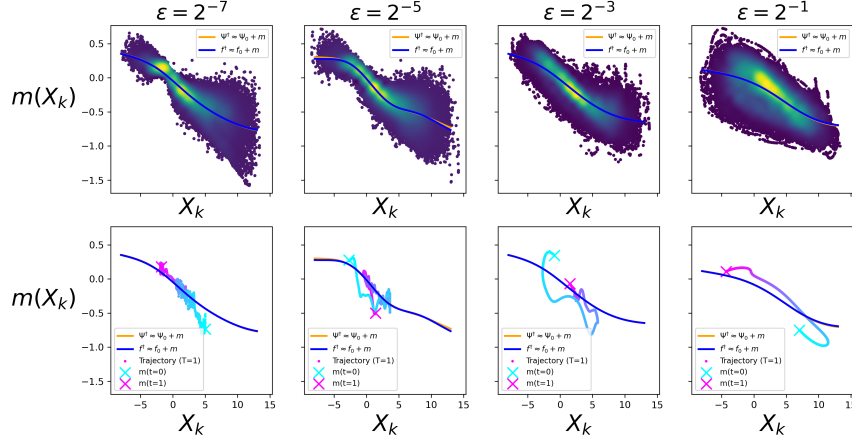


FIGURE 9. This figure shows the observed and estimated residuals of the nominal physics model f_0 for the Lorenz '96 Multiscale system at different scale-separation factors. The first row shows the density of these residuals (yellow is high density, blue is low), as well as the fit of our closure terms in continuous- (blue) and discrete- (orange) time. We see that the small timestep of $\Delta t = 0.001$ makes the discrete case behave similar to learning Euler increments (we have normalized the discrete model by dividing by Δt to show this here). For larger ε , we see increasing variance of the residuals around our estimate. Furthermore, the second row shows temporal structure in the errors of our residual fit by superimposing a short ($T=1$) one-dimensional trajectory (this represents roughly 0.1% of the training data). For large scale-separation (left), the true residuals oscillate rapidly around our Markovian fit. For small scale-separation (right), the true residuals have substantial structure in their deviations from the residual fit; in cases like these, a memory-based residual may be able to target these deviations.

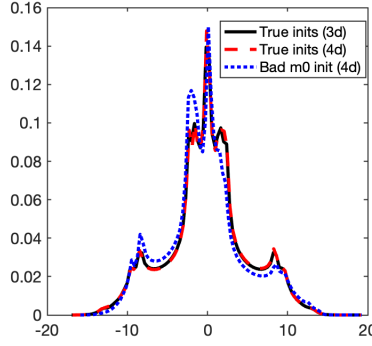


FIGURE 10. Here, we show that the invariant density for the first component of Lorenz '63 (black) can be reproduced by a correctly initialized augmented 4-d system (dashed red) in eq. (6.4). However, incorrect initialization of $m(0)$ in eq. (6.4) (dotted blue) yields a different invariant density.

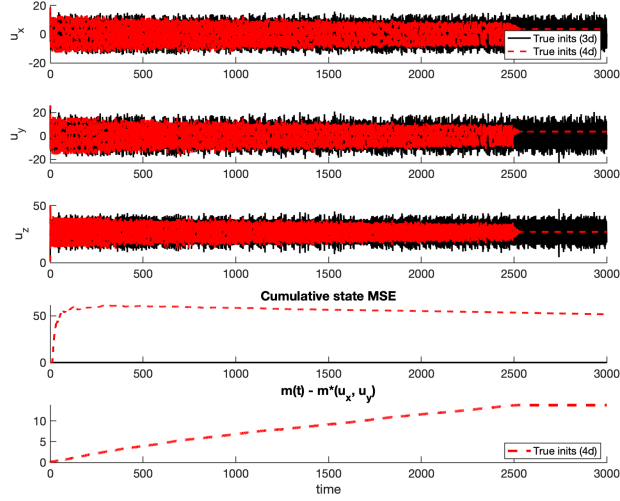


FIGURE 11. Here we show that the embedded 3-dimensional manifold of Lorenz 63, within the 4-dimensional system given by eq. (6.5), is unstable. Indeed the correctly initialized 4-dimensional system (dashed red) has solution which decays to a fixed point. The bottom figure shows divergence of the numerically integrated model error term $m(t)$ and the state-dependent term m^\dagger ; this growing discrepancy is likely responsible for the eventual collapse of the 4-dimensional system.

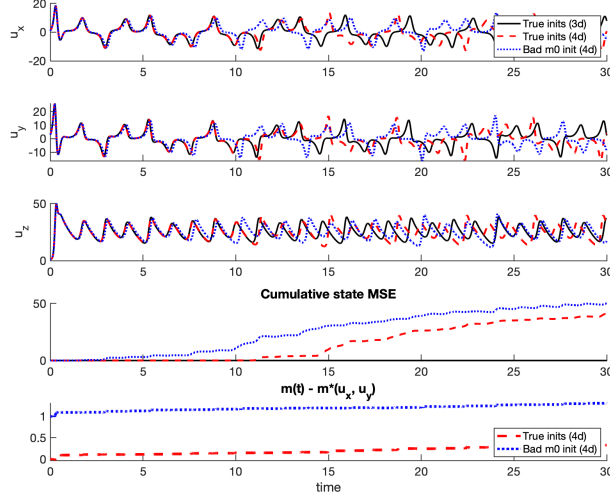


FIGURE 12. Here, we show short-term accuracy for the 4-dimensional system in eq. (6.5). Predictions using the correct initialization of m_0 (dashed red) remain accurate for nearly twice as long as predictions that use a perturbed initialization ($m_0 = m^\dagger(u_x, u_y) + 1$). The bottom figure shows that $m(t)$ diverges from the state-dependent m^\dagger more quickly for the poorly initialized model, but in both cases errors accumulate over time.